




Advancements in functional tetrahedral DNA nanostructures for multi-biomarker biosensing: Applications in disease diagnosis, food safety, and environmental monitoring

Yun Qiu^{a,1}, Yixing Qiu^{a,1}, Wenchao Zhou^a, Dai Lu^a, Huizhen Wang^a, Bin Li^a, Bin Liu^{b,**}, Wei Wang^{a,*} 

^a TCM and Ethnomedicine Innovation & Development International Laboratory, Academician Atta-ur-Rahman Belt and Road Traditional Medicine Research Center, School of Pharmacy, Hunan University of Chinese Medicine, Changsha, 410208, China

^b College of Biology, Hunan University, Changsha, 410082, China

ARTICLE INFO

Keywords:

Functional tetrahedral DNA nanostructure
Biomarker
Biosensing
Applications

ABSTRACT

Deoxyribonucleic acid (DNA) offers the fundamental building blocks for the precisely controlled assemblies due to its inherent self-assembly and programmability. The tetrahedral DNA nanostructure (TDN) stands out as a widely utilized nanostructure, attracting attention for its high biostability, excellent biocompatibility, and versatile modification sites. The capability of DNA tetrahedron to interact with various signal outputs makes it ideal for developing functional DNA nanostructures in biosensing platforms. This review highlights recent advancements in functional tetrahedral DNA nanostructures (FTDN) for various biomarkers monitoring, including nucleic acid, protein, mycotoxin, agent, and metal ion. Additionally, it discusses the potential of FTDN in the fields of disease diagnosis, food safety, and environmental monitoring. The review also introduces the application of FTDN-based biosensors for simultaneous identification of multiple biomarkers. Finally, challenges and prospects are addressed to provide guidance for the continued development of FTDN-based biosensing platforms.

1. Introduction

In recent years, biosensing has garnered widespread attention owing to its broad applications in environmental monitoring, food safety, disease diagnosis [1,2]. Especially, by converting biological signals into visible ones, biosensors have undergone extensive development for the analysis of nucleic acid, protein, enzyme, metal ion and other molecules [3–5]. Deoxyribonucleic acid (DNA), beyond being a genetic information carrier, also plays an indispensable role in the field of nanotechnology. The exceptional programmability and precise molecular recognition capability of DNA make it an excellent material for creating various functionalized DNA nanostructures, for instance, DNA origami, DNA hydrogel, cube, tetrahedron, octahedron, etc. These intricate nanostructures possess structural rigidity, high cellular uptake efficiency, and sufficient biostability, which are crucial for the construction of effective biosensors [6].

The tetrahedral DNA nanostructure (TDN), as a representative three-

dimensional (3D) nanostructure with multiple arms, has experienced significant advancements over the past two decades (Fig. 1). It was originally proposed by Turberfield in 2005 [7]. The self-assembly of TDN is achieved through Watson-Crick base pairing of four single-stranded DNAs [8] (Fig. 2). Through caveolin-mediated endocytosis, TDN is capable of entering cells and maintains stability for at least several hours, exhibiting resistance to nuclease degradation [9]. Furthermore, their exceptional editability and rich molecular modification capabilities make TDNs ideal for developing functionalized nanostructure known as functional TDN (FTDN) (Fig. 3). In biosensors construction, the highly stable and rigid TDN scaffold serves as a core and four vertices of which could be modified with functional nucleic acids and suitable nanomaterials, thereby facilitating interactions with multi-biomarkers, including nucleic acid, protein, mycotoxin, agent, and metal ion, etc. For instance, capture probes are modified at the TDN vertex to specifically recognize DNAs or RNAs (Fig. 3a). Antibody-modified TDN is utilized for antigen detection through specific

* Corresponding author. School of Pharmacy, Hunan University of Chinese Medicine, Changsha, 410208, China.

** Corresponding author.

E-mail addresses: binliu2001@hotmail.com (B. Liu), wangwei402@hotmail.com (W. Wang).

¹ These authors have contributed equally to this work.

antigen-antibody interactions (Fig. 3b). Furthermore, TDN-supported fluorescent biosensors are commonly used for intracellular enzymes sensing by incorporating enzyme recognition sites into the capture probe of the TDN (Fig. 3d). Metal-dependent DNAzymes can be incorporated into TDN for the detection of metal ions (Fig. 3e). Aptamers anchored at the TDN vertex allow for capture cells (Fig. 3c), agents (Fig. 3f), and mycotoxins (Fig. 3g). In addition to functional nucleic acids, various nanomaterials are combined with TDN to enhance the sensitivity of the biosensing platform. These include gold nanoparticles (AuNPs), silver nanoparticles (AgNPs), reduced graphene oxide (rGO), covalent organic frameworks (co-MOFs), magnetic beads (MBs), quantum dots (QDs), and others.

The incorporation of such functional modifications makes TDN a versatile and powerful tool for multi-biomarker identification. This versatility underscores their significant potential in advancing disease diagnosis [10]. In the field of disease diagnosis, FTDN-based biosensors show tremendous potential for precise and speedy detection of disease-specific biomarkers. For instance, wang et al. [11] proposed a TDN-based nanosensor assisted with catalytic hairpin assembly (CHA) and CRISPR/Cas12a to detect exosomes, realizing early clinical diagnosis of non-small cell lung cancer (NSCLC). The combination of DNA tetrahedron significantly improves the capture efficiency of exosomes. Moreover, FTDN finds applications in ensuring food safety by detecting contaminants like mycotoxins and agents, thereby facilitating quality control. A recent proposal introduced FTDN nanotweezer combined with streptavidin magnetic nanoparticles for mycotoxins detection in cornmeal and rice, showcasing its potential for food safety monitoring [12]. Furthermore, it contributes to environmental monitoring by detecting pollutants such as metal ions and monitoring ecological health. Pei's group developed a TDN-functionalized microarray capable of simultaneously detecting Hg^{2+} , Ag^+ , Pb^{2+} within just 5 min [13]. This innovative approach successfully identified these metal ions in contaminated river water samples.

Since the first proposal of electrochemical biosensors by Fan's team in 2010 [14], FTDN-based biosensing platforms have been developed. These platforms offer promising capabilities for the synchronous detection of multiple biomarkers, which paves the way for comprehensive diagnostic applications. This review offers an in-depth overview of FTDN-based biosensors, emphasizing their effectiveness in detecting multi-biomarkers. It discusses the various strategies employed in the design and optimization of these biosensors to enhance their performance and reliability. Furthermore, the review highlights the current

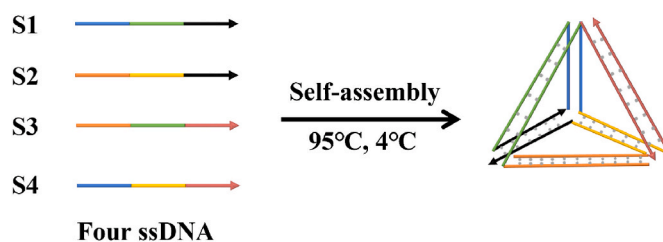


Fig. 2. Schematic diagram of self-assembled TDN.

challenges and future prospects of FTDN in biosensing and other biomedical fields, thus enhancing the functionality and expanding the practical applications.

2. Biosensing applications

2.1. Nucleic acid detection

Nucleic acids, including DNA and RNA, are nucleotide-based biopolymers responsible for storing and expressing genetic information, playing pivotal roles in cellular functions and diseases. Sensitive analysis of nucleic acids, including DNA, microRNA, and mRNA, is crucial for biomedical research and disease diagnosis. Currently, various techniques, such as northern blotting, microarrays, and quantitative reverse transcription PCR, are widely used for nucleic acid detection [15]. However, these traditional methods often face limitations due to the need for sophisticated equipment, intricate procedures, and high costs. Moreover, effective dynamic monitoring and regulation of intracellular nucleic acids demand strategies with improved biocompatibility. The rapid advancements in nanotechnology have unlocked new opportunities for biosensor construction [16]. Among these, TDN stand out as an excellent option, offering advantages such as rapid processing, cost-effectiveness, and compatibility with real-time imaging in living cells [17,18]. To date, numerous TDN-based nanosensors have been developed for sensitive bioanalysis of DNA, miRNA, and mRNA (Table 1).

2.1.1. DNA detection

Sequence-specific DNA is associated with genotypic and structural abnormalities. Sensitive and accurate specific DNA detection is crucial for genomic mutation analysis and early disease diagnosis [19–21]. TDN

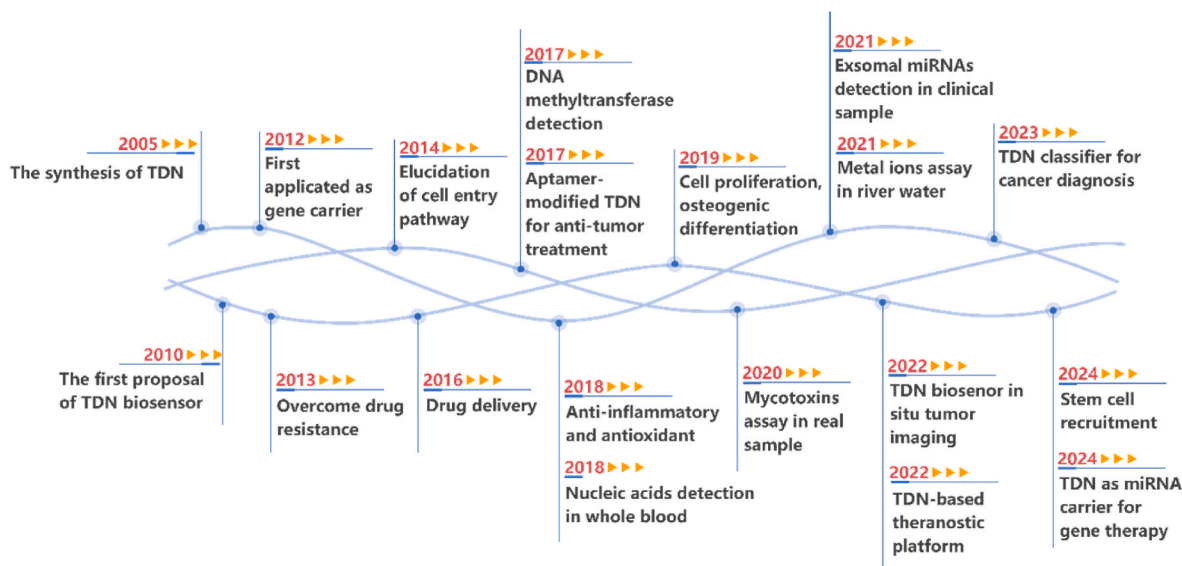


Fig. 1. The development of TDN over the past two decades.

is often combined with electrochemical technique for the detection of DNA [22]. Various nucleic acid amplification techniques, such as rolling circle amplification (RCA) and hybridization chain reaction (HCR), have been combined with TDN to enhance sensitivity [23]. Methylated DNA is a crucial epigenetic modification associated with genetic diseases and cancers. Zheng et al. [24] introduced an electrochemical strategy utilizing HCR and TDN for the detection of methylated DNA (Fig. 4A). In this approach, the TDN was integrated with a capture probe at one vertex. Two HCR hairpins were modified with biotin. The presence of methylated DNA triggered the production of numerous HCR products with the aid of *HpaII* endonucleases. Subsequently, horseradish peroxidase (HRP) induced a redox reaction to generate electrochemical signals. The incorporation of TDN enhanced the capture efficiency of methylated DNA while reducing nonspecific target adsorption. This electrochemical platform demonstrated a limit of detection (LOD) of 0.93 aM for DNA methylation. Moreover, the size of TDN can significantly influence the efficiency of DNA detection. Yuan's group developed a TDN electrochemical biosensor for the detection of p53 DNA based on enzyme cascade reactions [25] (Fig. 4B). In this study, the TDN was precisely designed to regulate the distance between the enzymes HRP and glucose oxidase (GOx). The TDN containing 30 base pairs was optimized to achieve the highest enzymatic catalytic efficiency. When p53 DNA was present, it initiated an exonuclease III (Exo III)-assisted cycling amplification strategy, resulting in the release of numerous

DNAzyme strands (DNA2). The DNA2 subsequently cleaved the TDN substrate in the presence of Pb^{2+} , releasing enzyme-modified segments. Upon the addition of glucose, a significant electrochemical response was observed. This TDN scaffold provided valuable insights into enhancing the efficiency of enzyme cascade reactions through controlled TDN design. In another study, the red blood cells with good biocompatibility were utilized to attach with TDN, realizing efficient capture of circulating tumor DNA (ctDNA) [26] (Fig. 4C). Four TDN were designed with different DNA2 chains, while the red blood cells were integrated with DNA1. The ctDNA was recognized by both TDNs and red blood cells, enabling the formation of a DNA sandwich through complementary base pairing. Upon the addition of signal tags (methylene Blue), electrochemical signals were generated. This biocompatible biosensor demonstrated a LOD of 0.66 fM for ctDNA. Furthermore, the successful detection of serum ctDNA highlighted its potential for early cancer diagnosis. In addition to electrochemical biosensors, the use of carbon nanotube (CNT) transistors has emerged as a promising approach for ctDNA detection, offering exceptional sensitivity and selectivity. For the first time, a CNT thin-film transistor (CNT TFT) sensor was developed for the detection of AKT2 DNA [27]. The AKT2 DNA was hybridized with TDN, resulting in an increased drain current. The incorporation of TDN significantly improved the capture efficiency, achieving up to 98 % enhancement compared to single-stranded DNA probes. This nanosensor achieved an impressive LOD of 0.2 fM for AKT2 DNA, demonstrating

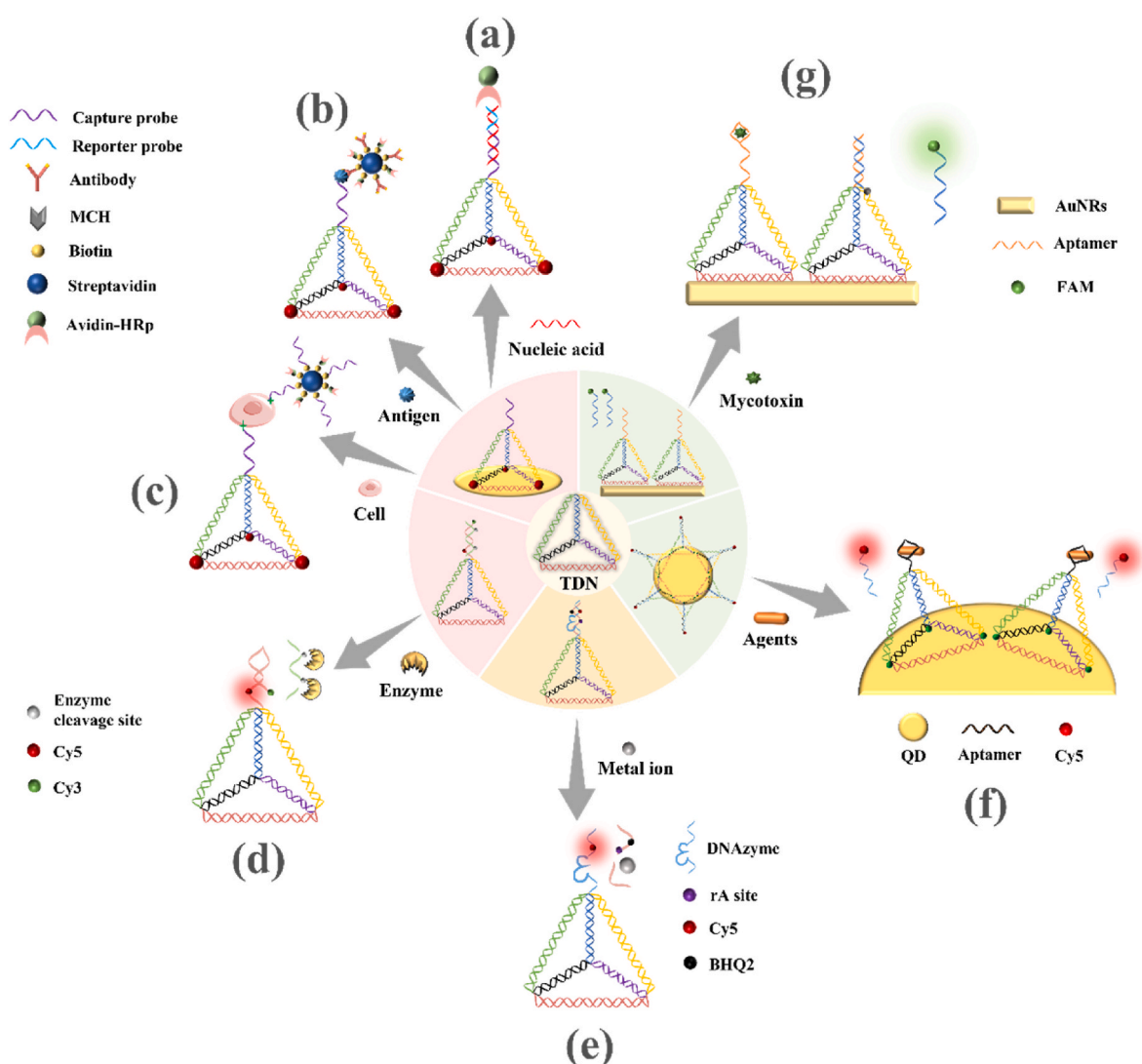


Fig. 3. Schematic diagram of TDN for multi-biomarker detection.

Table 1
FTDN-based biosensors for DNA detection.

Target	Method	Signal labeling	Detection Range	LOD	Publish year	Ref.
DNA methylation	Electrochemical	Hemin/G-quadruplex HRP-mimicking DNAzyme	10 pM to 10 nM	0.1 fM	2018	[23]
DNA methylation	Electrochemical	TMB/HRP	1 aM to 100 nM	0.93aM	2019	[24]
P53 gene	Electrochemical	TMB/HRP and GOx	0. 01 pM to 10 nM	3 fM	2019	[25]
ctDNA	Electrochemical	Methylene blue	1 fM to 100 pM	0.66 fM	2023	[26]
AKT2 gene	All-CNT TFT	CNT/N-(1-pyrenyl) maleimide	1 pM to 1 μM	2 fM	2022	[27]
COVID DNA	ECL	PEI-Ru@Ti ₃ C ₂ @AuNPs-S7	10 aM to 10 pM	7. 8 aM	2022	[32]

(The detection range: The concentration range within which a method can accurately identify and quantify a target, reflecting the method's effective operation with precision and reliability. LOD: The limit of detection, the lowest concentration reliably detectable under defined conditions, representing the smallest signal distinguishable from background noise with statistical significance.)

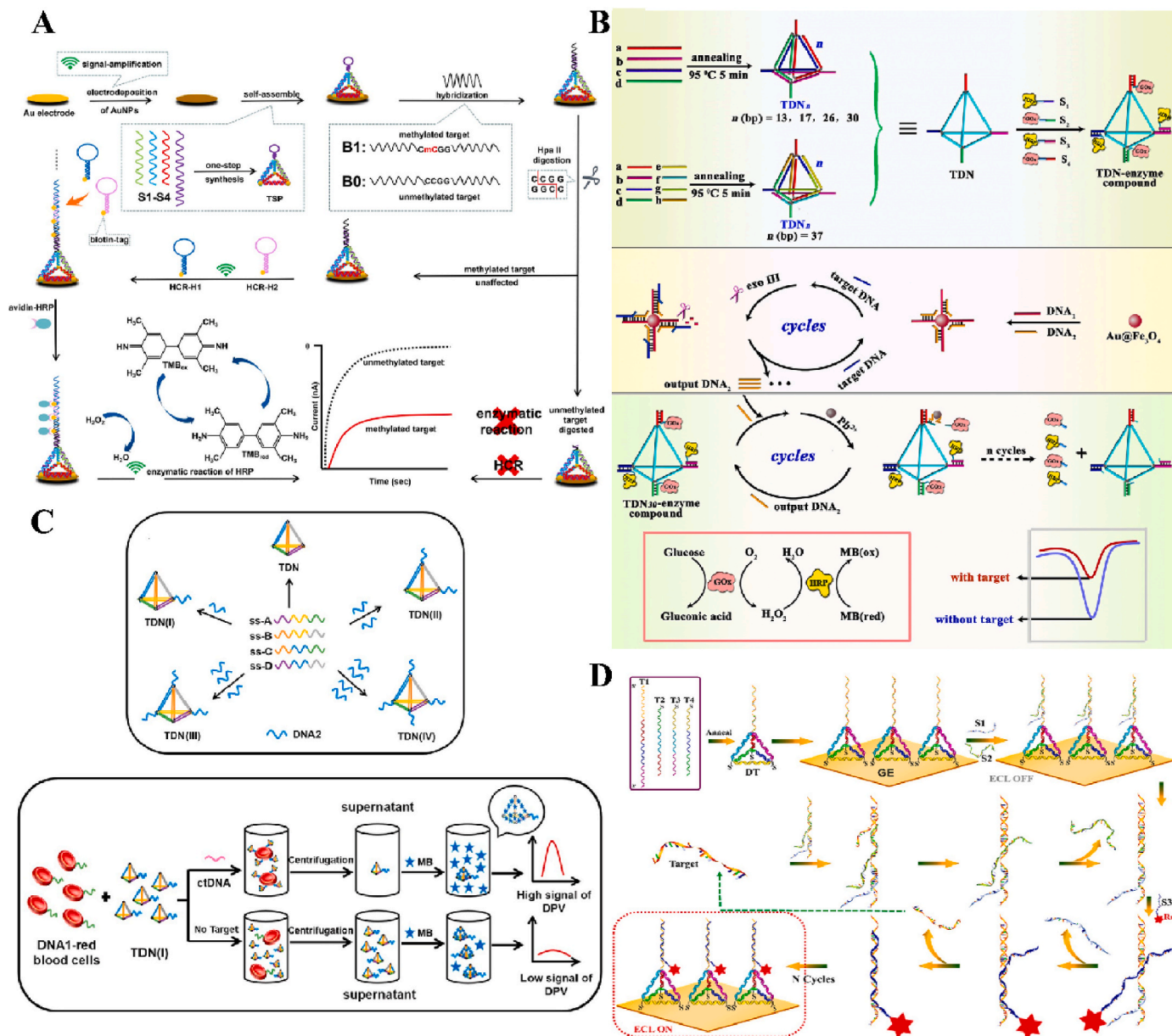


Fig. 4. Schematic illustration of TDN based electrochemical biosensors for DNA detection. (A) An electrochemical biosensor combined with TDN and HCR for determination of DNA methylation. Reprinted from Ref. [24]. Copyright 2019, American Chemical Society. (B) A TDN based electrochemical biosensor for p53 DNA identification through precise regulation of inter-enzyme reactions. Reprinted from Ref. [25]. Copyright 2019, American Chemical Society. (C) A biocompatibility electrochemical biosensing platform integrating TDN and red blood cells for ctDNA detection. Reprinted from Ref. [26]. Copyright 2022, Elsevier. (D) An ECL strategy involving TDN for sensitive RdRp-COVID DNA analysis. Reprinted from Ref. [33]. Copyright 2021, Elsevier.

considerable potential for the diagnosis of triple-negative breast cancer.

Bioanalysis of nucleic acids is essential for virus-related diseases diagnosis, including coronavirus disease 2019 (COVID-19) [28], acquired immune deficiency syndrome (AIDS) [29], as well as cervical cancer [30]. Developing portable, fast, and cost-efficient nucleic acid analysis platforms is crucial. Various techniques, such as field-effect transistor (FET) and Electrochemiluminescence (ECL), have been applied to develop TDN-based biosensing platforms for the detection of viral nucleic acids [31,32]. ECL is an emerging biosensing technology that combines luminescence and electrochemical methods for nucleic acid-based sensors. Zhang's group developed an ECL strategy utilizing TDN for the sensitive profiling of RNA-dependent RNA polymerase (RdRp)-COVID DNA [33] (Fig. 4D). The presence of RdRp-COVID DNA initiated an entropy-driven reaction that enabled the signal tag (Ru)-labeled S3 to connect with the linear single-stranded DNA at the vertex of the TDN. The proximity of Ru to the gold electrode triggered an ECL "signal-on" state, facilitating signal amplification through cycles of released RdRp-COVID DNA. The use of TDN prevented cross-reactivity among single-stranded DNA, thereby enhancing the ECL intensity. This method successfully detected RdRp-COVID in human serum samples, providing a reliable and feasible sensing platform for clinical bioanalysis.

2.1.2. microRNA detection

MicroRNAs (miRNAs), as the most studied non-coding RNA molecules, are critical for regulating target gene expression and influencing cellular signaling pathways. Abnormal miRNA regulation is linked to various diseases, including cancer, cardiovascular conditions, inflammation, and neurological disorders [34]. Sensitive miRNA detection plays a vital role in early disease diagnosis and prognosis, particularly in cancer [35]. However, challenges such as low miRNA abundance and complex biological systems can lead to false positives. Research shows that TDN-supported biosensing platforms offer high sensitivity and anti-interference for miRNA quantification [36–38]. Herein, we provide an overview of TDN for detecting extracellular (Table 2) and intracellular miRNAs (Table 3).

2.1.2.1. Extracellular detection. Numerous biosensing platforms utilizing fluorescent, electrochemical, and ratiometric technologies have been developed for the sensitive detection of miRNAs, offering promising prospects for cancer diagnosis. To overcome the challenges of nuclease degradation, an anti-interference TDN-based fluorescent biosensor was proposed for the detection of miRNA-21 [39] (Fig. 5A). Unlike single-stranded DNA, the TDN's with structural stability transformed the nuclease into a catalyst. This nanodevice showed strong resistance to degradation in the absence of miRNA-21, minimizing false

positives. When miRNA-21 is present, the TDN underwent conformational changes, facilitating catalysis and releasing a FAM-labeled strand that generated a fluorescent signal. This stabilized nanodevice achieved a 700 % signal enhancement within 2 h at room temperature and nearly a 10-fold reduction in LOD under biomimetic conditions. Its successful application in detecting serum miRNA-21 in colorectal cancer patients underscored the potential of TDN biosensors for early cancer diagnosis. Exosomal microRNAs (exo-miRNAs) are released at high levels by various tumor cells, making their detection vital for cancer diagnosis and treatment. Recently, a ratiometric sensor incorporating a TDN and CHA was developed for the visual detection of exo-microRNA-150-5p [40] (Fig. 5B). The lateral flow test strip provided a promising platform for miRNA identification by forming visual lines or spots. The TDNs were distributed at the strip as capture probes. Exo-microRNA-150-5p facilitated the formation of stable double-strands, initiating CHA assembly and hybridizing with barcoded TDNs, which then attached to streptavidin-coated gold nanoparticles (SA-AuNPs). This resulted in a red line, while unbound SA-AuNPs were captured on the control line, thereby producing a ratiometric response. TDNs prevented the displacement during flow and enhancing detection reliability with a LOD of 58.90 fM for exo-microRNA-150-5p. The electrochemical technique is widely employed for miRNA detection due to its rapid signal readout capability. Qiu et al. [41] proposed an electrochemical biosensor combining TDN and CHA for exo-miRNA profiling (Fig. 5C). In the presence of exo-miRNA, two TDNs (T1 and T2) incorporated CHA hairpin structures, inducing intramolecular CHA (intra-CHA). This resulted in the loading of RuHex onto the TDNs, achieving the amplified detection of exo-miRNA with a LOD of 7.2 aM within 30 min. The platform exhibited 90.5 % sensitivity for breast cancer diagnosis by detecting four exo-miRNA-1246, exo-miRNA-221, exo-miRNA-375, and exo-miRNA-21. CRISPR/Cas13a, a novel endonuclease with trans-cleavage capability, is widely employed in nucleic acid biosensing. Mi et al. [42] introduced an electrochemical biosensor combining TDN with the CRISPR/Cas13a system for detecting microRNA-19b (miRNA-19b) (Fig. 5D). This configuration featured TDN integrated with an RNA reporter and avidin-HRP as the signal reporter. The hybridization of miRNA-19b with Cas13a activated its trans-cleavage capability, which led to the readout signal and eventually achieved a LOD of 10 pM in mimic serum. In addition to the classic single-readout method, the dual-output signal demonstrates significant superiority in enhancing detection capabilities, particularly in resisting environmental interference [43]. Herein, a dual-signal readout technology was developed for the ultrasensitive analysis of miRNA-21 [44]. The TDN was employed to enhance the loading capacity and binding efficiency of the miRNA. The TDN with a stem-loop structure hybridized with the miRNA-21, triggering HCR with hairpins labeled with Fc and MB. This dual-signal

Table 2

FTDN-based biosensors for miRNA detection.

Target	Method	Signal labeling	Detection Range	LOD	Publish year	Ref.
miRNA-21	Fluorescent	Fluorophore	/	100 aM	2023	[39]
miRNA-21	Electrochemical	Ferrocene and methylene blue	50 fM to 100 pM	1.92 fM/3.74 fM	2022	[44]
miRNA-21	Electrochemical	Hemin/G-quadruplex HRP-mimicking DNAzyme	0.5 fM to 100 nM	0.04 fM	2019	[45]
miRNA-21	Electrochemical	Ferrocene	0.01 fM to 100 aM	0.25 fM	2020	[46]
miRNA-21	Electrochemical	Methylene blue	50 nM to 2 μM	19.8 aM	2023	[47]
Exo-miRNA-150-5p	Ratiometric	AuNPs	10 pM to 10 nM	58.90 fM	2023	[40]
Exo-miRNAs	Electrochemical	RuHex	10 aM to 100 μM	7.2 aM	2021	[41]
Exo-miRNA-21	Electrochemical	RuHex	100 aM to 1 nM	34 aM	2022	[48]
miRNA-19b	Electrochemical	TMB/HRP	0.01 pM to 10 fM	10 aM	2021	[42]
miRNA-155	ECL/AdsV	g-C ₃ N ₄ @AgNPs	0.01 to 10 pM/0.05 to 10 pM	50 fM/100 fM	2021	[49]
miRNA-155	Plasmonic	C=O bond	100 fM to 10 nM	0.1 pM	2021	[50]
mRNA-155	ICP-MS	AuNPs	0 to 20 nmol/L	1.15 pM	2021	[51]
miRNA-155	ECL	CuNCs	100 aM to 100 pM	36 aM	2018	[56]
miRNA-122	SERS	TB and AuNPs	0.01 aM to 10 fM	0.009 aM	2020	[52]
Hsa-miR-193a-3p	Electrochemical	TMB/HRP	0.1 fM to 1 nM	0.1 fM	2020	[53]
miRNA-141	Electrochemical	Methylene blue	10 aM to 100 pM	4.9 aM	2022	[54]
miRNA-182-5p	PEC	TiO ₂ /MIL-125-NH ₂ /Au/PWE	0.1 fM to 100 pM	0.09 fM	2023	[55]

Table 3
FTDN-based biosensors for intracellular miRNA detection.

Target	Method	Fluorophore	Detection Range	LOD	Living cells	Publish year	Ref.
miRNA-21	Fluorescent	FAM	1 pM to 200 nM	0.8 pM	MCF-7/HeLa/MRC-5 cells	2022	[63]
miRNA-21	Fluorescent	FAM	1 nM to 100 nM	2 pM	L02/HeLa/MCF-7 cells	2021	[64]
miRNA-let 7a	Fluorescent	FAM and TAMRA	0.5 to 25 nM	22.35 pM	MCF-7 cells	2021	[65]
miRNA-21	Fluorescent	FAM	1 nM to 100 nM	/	MCF-7/HepG2 cells	2018	[66]
miRNA-155	Fluorescent	Cy3 and Cy5	100 pM to 60 nM	120 pM	MCF-7/HeLa/MRC-5 cells	2022	[67]
miRNA-21	Fluorescent	Cy5 and FAM	/	/	A549/MCF-7/A375	2022	[68]
miRNA-21	Fluorescent	Cy3	30 pM to 50 nM	17.8 pM	MCF-7 cells	2019	[69]
miRNA-21	Fluorescent	FAM	1 pM to 1 μ M	0.77 pM	L02/HepG2 cells	2022	[70]

strategy improved the reliability and accuracy of serum miRNA-21 detection. More information on TDN biosensing platforms for miRNAs detection is briefly listed in Table 1 [45–55].

2.1.2.2. Intracellular detection. Real-time monitoring of miRNAs plays a pivotal role in revealing their dynamic changes and intracellular distribution, which enhances our knowledge of their physiological roles [57,58]. Fluorescent methods are extensively employed for this purpose due to their high sensitivity and operational simplicity [59,60]. TDN can enter cells through caveolin-mediated endocytosis, enabling its use in monitoring intracellular targets. Until now, a variety of TDN-based fluorescent biosensors have been proposed for sensitive and accurate miRNAs identification at the subcellular level [61,62]. According to researches, the majority of TDN-based nanoprobe for intracellular miRNAs rely on fluorescence resonance energy transfer (FRET) [63–65]. AuNPs have been incorporated into fluorescent biosensing platforms due to their exceptional fluorescence quenching ability and large surface area. For example, a FRET-based fluorescent biosensor based on TDN and AuNPs was developed for the monitoring of miRNA-21 [66] (Fig. 6A). When the miRNA-21 is present, the fluorophore-modified strand dissociated from AuNPs, generating a strong fluorescence signal. This method successfully visualized miRNA-21 in cancer cells. The assembly of polymeric TDNs triggered by miRNAs offered an optimal approach for amplified miRNA imaging [67]. Lin' group developed a TDN nanoprobe based on HCR for rapid monitoring of miRNA-21 and nucleolin [68] (Fig. 6B). When these TDNs encountered cancer cells, the overexpressed miR-21 initiated the intra-HCR process and resulted in the formation of polymeric TDNs. The HCR-TDN nanosensor exhibited detection rates three times faster than free HCR reaction. More importantly, this system showcased *in vivo* fluorescence signals within 15 s post tumor injection. The probe's successful application for *in situ* tumor imaging underscoring its potential for clinical cancer diagnosis. In addition to the AuNPs and fluorophore, near-infrared (NIR) light provides a new option for powering the miRNA imaging. Pang et al. [69] proposed a novel strategy to track miRNA-21 in live cells using TDN-based nanomachines powered by 808 nm NIR light. This system converted NIR photons into ultraviolet photons, activating a toehold strand displacement reaction that restored fluorescence due to a "FRET off" state. This NIR-powered nanomachine effectively monitored miRNA-21 fluctuations in cancer cells.

The simultaneous determination and regulation of miRNA plays an important role in early cancer diagnosis and treatment but poses significant challenges. Zhang's team developed a DNA tetrahedral nanomachine, featuring an allosteric DNAzyme controlled by miRNA-21 inhibitors [70] (Fig. 6C). This nanomachine enabled sensitive intracellular detection and negative feedback regulation of miRNA-21. With the aid of miRNA-21, the locked tetrahedral DNAzyme underwent conformational changes to its active form, cleaving the specific site rA and increasing spatial separation between FAM and BHQ-1, thus restoring the fluorescent signal. This tool effectively regulated intracellular miRNA-21 levels by inhibiting miRNA-mRNA interactions, offering a novel platform for miRNA analysis and regulation.

2.1.3. mRNA detection

Messenger RNA (mRNA), a single-stranded RNA produced during DNA transcription, acts as a template for protein translation and is vital in various biological processes. Differential mRNA level in cells is linked to cellular proliferation and tumor progression [71]. Due to the excellent biocompatibility and biostability of TDN, various TDN-based biosensors have been developed for the detection of endogenous mRNAs [72–74] (Table 4). In one study, a novel intra-CHA-TDN nanoprobe was devised for the imaging of MnSOD mRNA in living cells [75] (Fig. 7A). The TDN served as a structural scaffold for two hairpin structures that incorporated fluorophores. Upon the presence of MnSOD mRNA, the CHA mechanism was activated, resulting in the reduction of the distance between the two fluorophores to a level conducive for efficient FRET, thereby producing a fluorescent signal. Notably, when compared to traditional free-CHA methodologies, the intra-CHA-TDN system exhibited a remarkable 15.6-fold enhancement in signal generation rate. Advancements in mRNA detection have provided a powerful tool for cancer diagnosis. Sun et al. developed a TDN-based thermophoretic strategy for imaging prostate-specific antigen (PSA) mRNA in extracellular vesicles (EVs) [76] (Fig. 7B). The TDN, modified with two fluorophore-labeled strands, took advantage of its efficient internalization by EVs. In the presence of PSA mRNA, the two fluorophore-labeled probes of TDN bound to the mRNA, resulting in an increased FRET signal due to the close proximity of Cy3 and Cy5. Additionally, to further enhance the FRET signal, infrared laser-based thermophoretic accumulation was applied to EVs encapsulating TDN. This thermophoretic assay enabled ultrasensitive detection of serum PSA mRNA with a LOD of 14 aM. More importantly, it was capable of distinguishing between prostate cancer and benign prostatic hyperplasia.

2.2. Protein detection

The detection of cancer is significantly enhanced by identifying overexpressed proteins, which act as biomarkers indicative of malignant transformation, thereby facilitating targeted diagnostic approaches [77, 78]. Notable examples include glycoproteins such as glycoproteins such as mucin 1 (MUC1), HER2, carcinoembryonic antigen (CEA), and prostate-specific antigen (PSA). The levels of these proteins are often significantly elevated in cancerous tissues or the bloodstream compared to normal physiological conditions [79]. As a result, the sensitive and convenient detection of these cancer biomarkers is essential for effective cancer monitoring and early diagnosis. Western blotting and enzyme-linked immunosorbent assay are widely used methods for protein quantification [80]. However, their complex procedures and moderate sensitivity limit their effectiveness for precise disease diagnosis. Recently, the extensive application of DNA nanomaterials in biomarker detection has highlighted TDN as a promising tool for protein assays [81]. TDNs facilitate the functional modification of antibodies, aptamers, and specific recognition sites, significantly improving protein capture efficiency. Furthermore, the integration of TDNs with various analytical techniques enhances detection sensitivity. In this section, we discuss the application of TDN-based biosensors for the identification of antigens (Table 5), cancer cells (Table 6), and enzymes (Table 7).

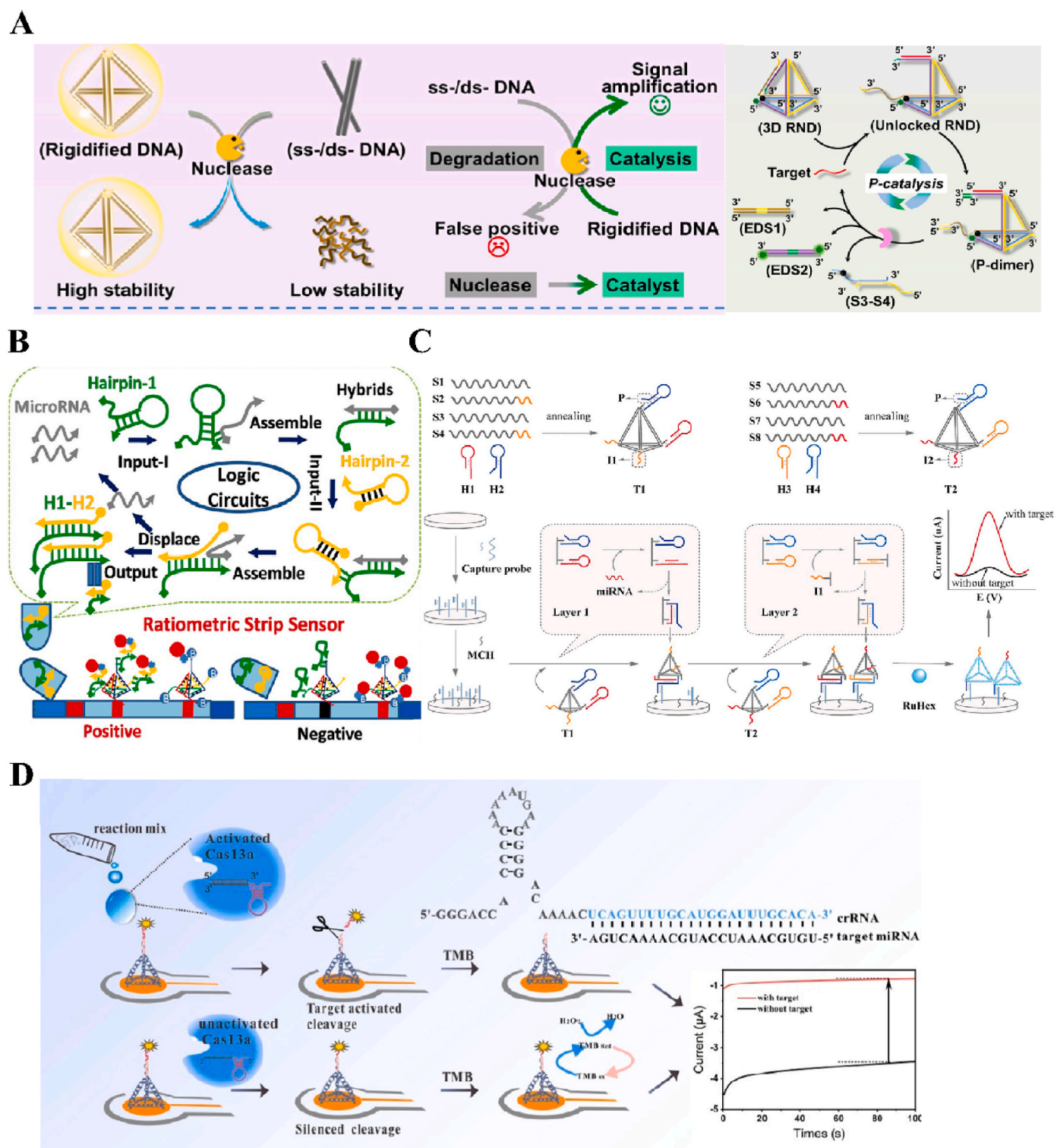


Fig. 5. Schematic illustration of TDN based nanosensor for extracellular miRNAs detection. (A) An anti-interference TDN-based fluorescent biosensor for miRNA biosensing by turning nuclease into a catalyst. Reprinted from Ref. [39], Copyright 2023, Elsevier. (B) A ratiometric strategy based on the TDN and CHA for the visual detection of exo-miRNA-150-5p. Reprinted from Ref. [40], Copyright 2023, Elsevier. (C) An electrochemical biosensor assisted with TDN and CHA for exo-miRNA-150-5p detection. Reprinted from Ref. [41], Copyright 2021, Elsevier. (D) TDN and the CRISPR/Cas13a system involved electrochemical strategy for miRNA-19b detection. Reprinted from Ref. [42], Copyright 2022, Elsevier.

2.2.1. Antibody based approaches

Based on antigen-antibody interactions, TDN immunosensors have been developed for protein detection [82,83]. Dai et al. designed a molybdenum disulfide (MoS_2) FET biosensor utilizing TDN for the ultrasensitive detection of PSA [84] (Fig. 8A). The TDN was integrated

with biotin, streptavidin, and anti-PSA, providing a stable platform for capturing PSA. In the presence of PSA, a TDN-involved PSA antibody-PSA nanostructure was formed. This study achieved a LOD of 1.0 fg/mL in phosphate-buffered saline, marking a 100-fold and 10,000-fold enhancement compared to previous studies.

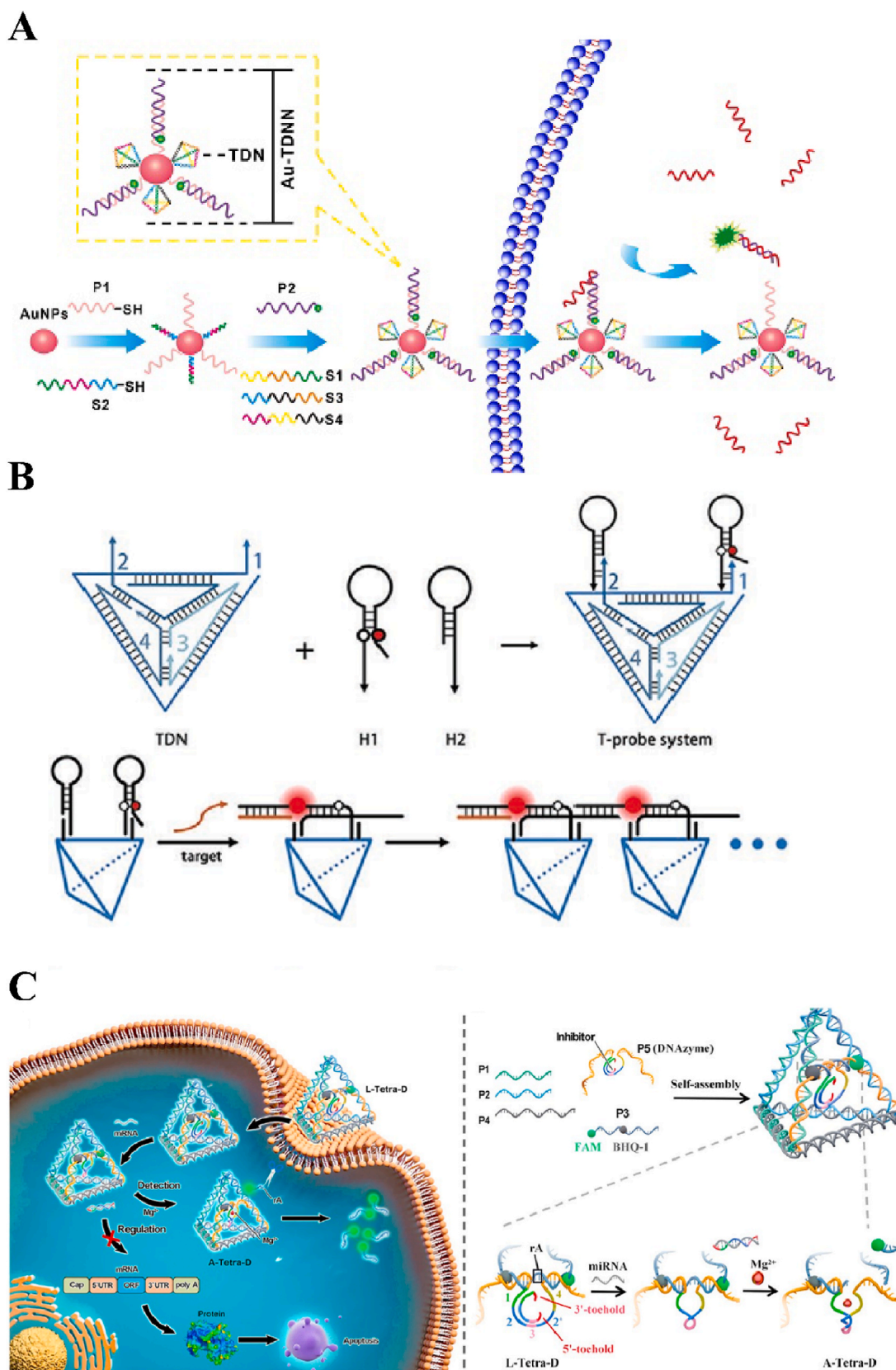


Fig. 6. Schematic illustration of TDN-based fluorescent biosensor for intracellular miRNAs detection. (A) A FRET-based fluorescent biosensor integrating AuNPs and TDN for miRNA-21 visualization. Reprinted from Ref. [66]. Copyright 2018, Ivyspring international publisher. (B) The assembly of polymeric TDN triggered by HCR for miRNA-21 imaging. Reprinted from Ref. [68]. Copyright 2022, John Wiley and Sons. (C) An allosteric DNAzyme controlled by miRNA-21 inhibitors for simultaneous imaging and regulation of miRNA-21. Reprinted from Ref. [70]. Copyright 2022, Elsevier.

Table 4

FTDN-based biosensors for mRNA detection.

Target	Method	Fluorophore	Detection Range	LOD	Living cells	Publish year	Ref.
TK1 mRNA	Fluorescence	Cy3 and Cy5	2 nM to 100 nM	0.33 nM	HepG2/HL7702 cells	2017	[72]
MnSOD mRNA	Fluorescence	Cy3 and Cy5	0.5 nM to 20 nM	3.5 pM	HeLa/MCF-7 cells	2020	[73]
MnSOD mRNA	Fluorescence	Cy3 and Cy5	0 to 100 nM	0.15 nM	L02/MDA-MB-231/MCF-7 cells	2019	[75]
Dll4 mRNA	Fluorescence	6-FAM and TEX615	0 to 1 μ M	30 pM	MCF7 cells	2020	[74]
PSA mRNA	Fluorescence	Cy3 and Cy5	10 pM to 100 nM	14 aM	/	2021	[76]

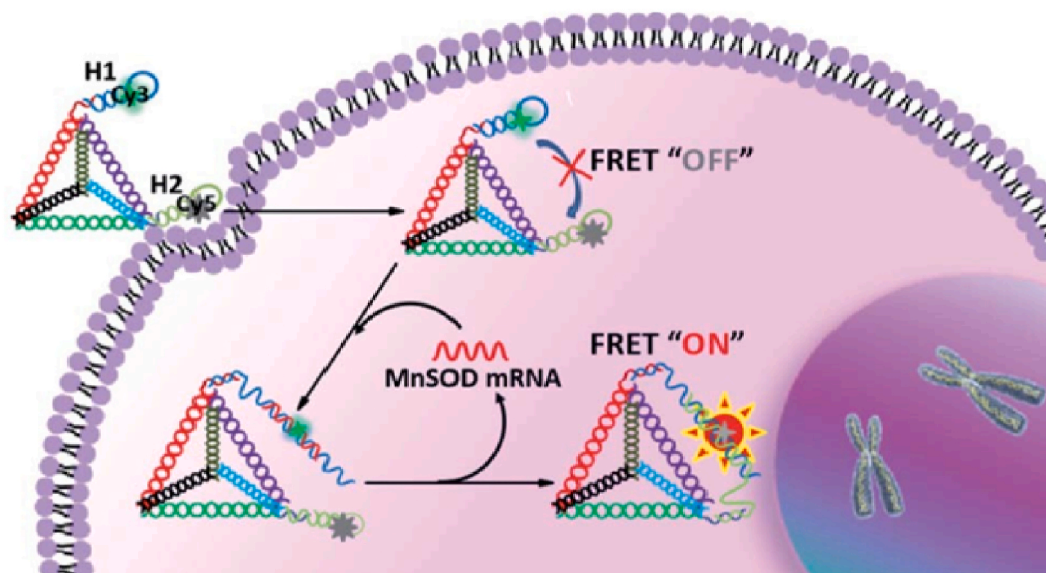
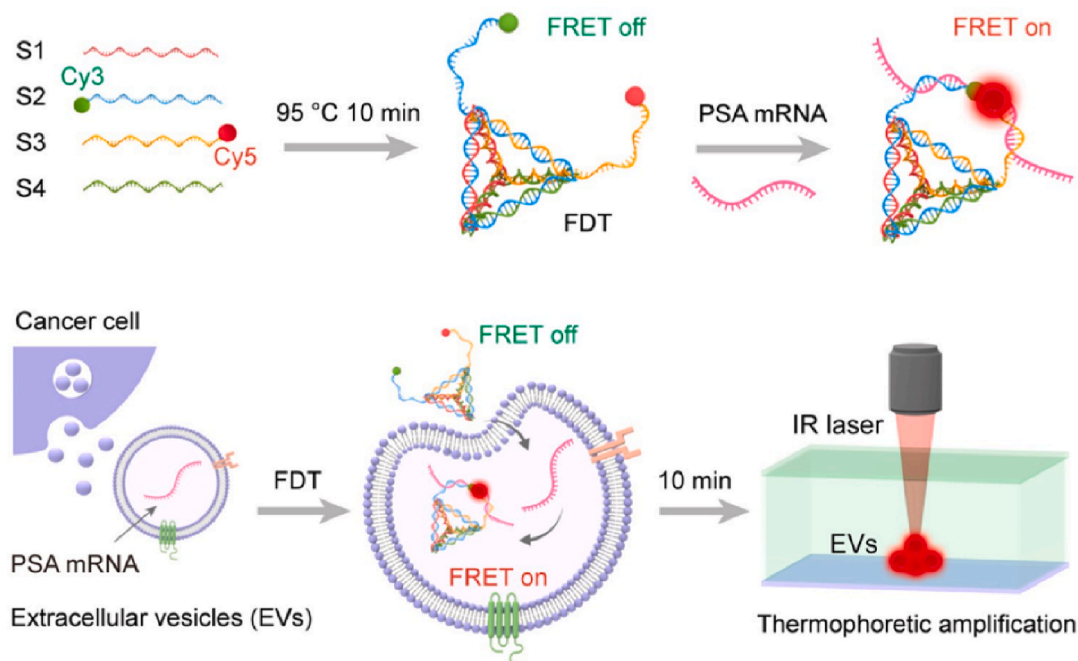
A**B**

Fig. 7. Schematic illustration of TDN-based fluorescent biosensing platform for intracellular mRNAs detection. (A) An intra-CHA based TDN nanoprobe for MnSOD mRNA imaging. Reprinted from Ref. [75]. Copyright 2020, Royal Society of Chemistry. (B) A TDN-based thermophoretic assay for EVs PSA mRNA monitoring in situ. Reprinted from Ref. [76]. Copyright 2021, Elsevier.

Table 5
FTDN-based biosensors for protein detection.

Target	Method	Signal labeling	Detection Range	LOD	Publish year	Ref.
PSA	Electrochemical	TMB/HRP	1 ng/mL to 100 ng/mL	0.2 ng/mL	2021	[83]
PSA	FET	MoS ₂	1 fg/mL to 100 ng/mL	1 fg/mL	2021	[84]
PSA	Electrochemical	Methylene blue	0.5 pg/mL to 50 ng/mL	0.15 pg/mL	2018	[85]
PSA	Electrochemical	AgNPs	1 pg/mL to 800 ng/mL	0.11 pg/mL	2018	[86]
HER2	Electrochemical	HRP	10 to 200 ng/mL	0.15 ng/mL	2019	[87]
Thrombin	Electrochemical	HRP	0.1 fM to 100 pM	35 fM	2020	[88]
Thrombin	Electrochemical	HRP	0.1 pM to 10 nM	11.6 fM	2018	[89]
Thrombin	Ratiometric electrochemical	[Fe(CN) ₆] ^{3-/4-} /Fe-MOFs	0.1 ng/mL to 50 ng/mL	59.6 fM	2020	[90]
Mucin 1	Electrochemical	Co-MOFs/thionine	4 fM to 400 pM	1.34 fM	2022	[91]
Exosomes	Electrochemical	Polydopamine	10 ² to 10 ⁷ particles/mL	1.39×10 ² particles/mL (EIS) and 6.27×10 ¹ particles/mL (DPV)	2024	[92]

Table 6
FTDN-based biosensors for cancer cell detection.

Target	Method	Signal labeling	Detection Range	LOD	Publish year	Ref.
MCF-7 cells	Electrochemical	HRP	0 to 10 ⁵ cells	1 cell	2021	[93]
MCF-7 cells	Fluorescence	AgNR	1 to 100 cells	1 cell	2022	[95]
MCF-7 cells	Electrochemical	Methylene blue	50 to 10 ⁶ cells/mL	5 cells	2020	[96]
MCF-7 cells	Electrochemical	Hemin/G-quadruplex	100 to 50000 cell/mL	23 cell/mL	2022	[97]
MCF-7 cells	Electrochemical	HRP-mimicking GQH DNazymes	20 to 10 ⁷ cells/mL	6 cells/mL	2019	[99]
MCF-7 cells	Microfluidic chip	/	10 to 10 ³ cells	/	2022	[100]
Hela cells	Electrochemical	CdTe QDs	0 to 10 ⁵ cell/mL	7 cell/mL	2022	[98]
HepG2 cells	Electrochemical	/	0 to 10 ⁶ cells	/	2020	[94]

Table 7
FTDN-based biosensors for enzyme detection.

Target	Method	Signal labeling	Detection Range	LOD	Living cells	Publish year	Ref.
Dam MTase	Fluorescent	FAM	0.1 to 90 U/mL	0.045 U/mL	/	2017	[105]
Dam MTase	Fluorescent	FAM	0.002 to 100 U/mL	0.00036 U/mL	/	2021	[115]
APE1	Fluorescent	FAM	0.01 to 100 U/mL	0.00554 U/mL	Hela/MCF-7/MCF-10A cells	2022	[107]
APE1	Fluorescent	Cy3	5 to 80 pM	5 pM	A549/HEK-293 cells	2019	[108]
APE1	Fluorescent	FAM	0.01 to 40 U/mL	0.01 U/mL	Hela cell	2020	[114]
APE1	Fluorescent	Cy5	0.01 to 60 U/mL	0.0026 U/mL	Hela/HEK-293 cells	2022	[117]
8-OG DNA glycosylase	Fluorescent	Cy5	0.5 to 100 U/mL	0.2443 U/mL	MCF-7 cell	2023	[109]
8-OG DNA glycosylase	Fluorescent	FAM	1 to 200 U/mL	0.52 U/mL	A549 cell	2024	[116]
Telomerase	Fluorescent	Cy5	500 to 100000 cells	39 cells	Hela/MCF-7/HL-7702/HCT cells	2022	[110]
Telomerase	Fluorescent	AgNCs	50 to 1000 cells	1 cell	/	2022	[112]
RNAase H	Fluorescent	FAM	0.075 to 15 U/mL	0.01 U/mL	HepG2 cell	2021	[113]
RNAase A	Fluorescent	FAM	0.05 to 10 pg/μL	0.09 pg/μL	HepG2 cell	2020	[118]

2.2.2. Aptamer based approaches

Aptamers are RNA or DNA molecules that specifically bind to proteins. Aptamer-functionalized biosensors (aptasensors) are used for biomarker capture, offering advantages like high selectivity, rapid response, and low cost. TDN-based aptasensors exhibit higher sensitivity than single-stranded aptamer sensors for their structural rigidity [85, 86]. For instance, a dual-aptamer biosensor based on TDN was developed for the electrochemical analysis of HER2 [87] (Fig. 8B). The TDN was functionalized with the HB5 aptamer for specific recognition. The gold nanorod served as a platform for signal tags (Pd, HRP), and the HB5 aptamer. It facilitated the formation of the Gold Nanorods@Pd-Apt-HRP nanoprobe as both a capture and a signal probe. In the presence of HER2, a sandwich-type structure of TDN-HER2-nanoprobes was established on the gold electrode surface. This aptasensor demonstrated significant diagnostic potential with a detection limit of 0.15 ng/mL for HER2. Reduced graphene oxide (rGO), a derivative of graphene, is distinguished by its exceptional electrical and mechanical properties, as well as a high specific surface area. Furthermore, it offers superior biosafety compared to GO, making it an efficient and biocompatible material for electrochemical biosensor construction [88]. By immobilizing TDN on

an rGO-modified electrode, Wang's group developed a thrombin aptasensor that integrated TDN with HCR signal amplification strategy [89] (Fig. 8C). In this study, researchers introduced sulfur and nitrogen-doped reduced graphene oxide (SN-rGO), which significantly enhanced the catalytic activity of rGO. Thrombin was competitively captured by the aptamer, allowing the cDNA to hybridize with the TDN. Subsequently, in the presence of HCR hairpins, HCR was initiated on the TDN, resulting in a significant current response through the catalytic reaction. The biosensor demonstrated a low LOD for thrombin at 11.6 fM. Traditional TDN biosensors usually utilize a single signal input. Developing ratiometric methods has become a smart approach to enhance the reproducibility of biosensing [90]. Hu et al. [91] developed a ratiometric aptasensor based on metal-organic frameworks (MOFs) for the detection of MUC1 (Fig. 8D). MOFs are considered excellent signal tags due to the high surface areas and abundant metal ions. This study employed novel Co-MOFs to provide strong and stable electrochemical signals. In the presence of MUC1, a TDN-MUC1-DNA sandwich structure was formed on the electrode. Signal amplification was triggered by Co-MOFs-labeled HCR hairpins. The current signal from Co-MOFs was detected, while thionine was used as a reference upon the addition of

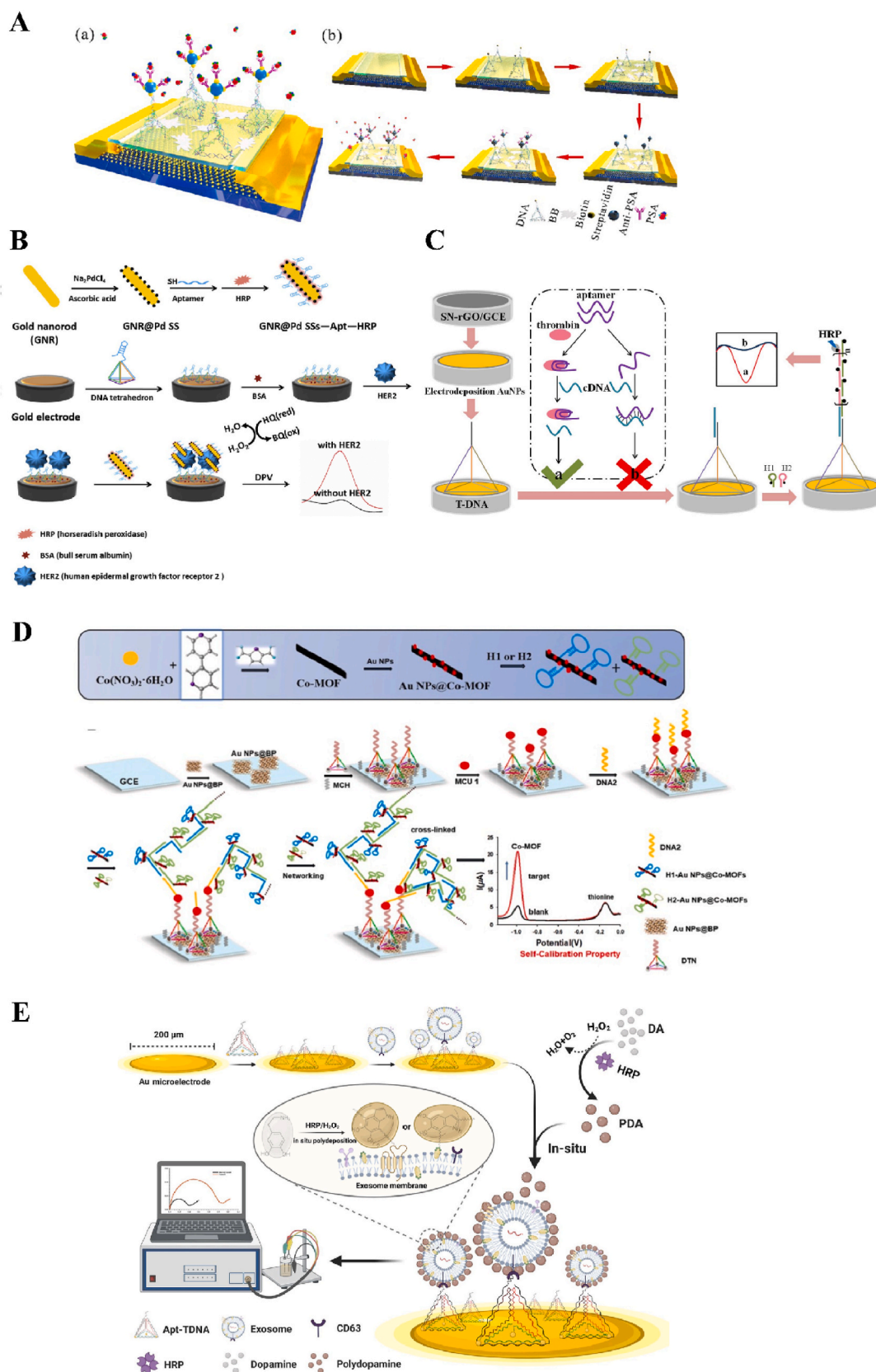


Fig. 8. Schematic illustration of TDN-based biosensors for protein detection. (A) MoS₂ FET biosensor based on TDN for ultrasensitive detection of PSA. Reprinted from Ref. [84]. Copyright 2021, Elsevier. (B) An electrochemical biosensor based on TDN with dual aptamers for HER2 bioanalysis. Reprinted from Ref. [87]. Copyright 2019, Elsevier. (C) A TDN aptasensor that integrated with HCR for thrombin detection. Reprinted from Ref. [89]. Copyright 2017, Elsevier. (D) A ratiometric TDN aptasensor based on MOFs for the detection of MUC1. Reprinted from Ref. [91]. Copyright 2022, Elsevier. (E) A PDA coated TDN aptasensor for the electrochemical identification of exosomes. Reprinted from Ref. [92]. Copyright 2024, Springer nature.

MUC1. This dual-signal ratiometric strategy achieved highly sensitive detection of MUC1 with a LOD of 1.34 fM. More importantly, the current ratio remained stable across ten different working electrodes, demonstrating the excellent stability of this ratiometric aptasensor.

Exosomes, carrying a wealth of biomolecules derived from tumors, are considered crucial cancer biomarkers. The highly sensitive analysis of exosomes shows significant potential for early cancer diagnosis. As the abundant membrane protein CD63 present on exosomes, researchers developed an electrochemical strategy that integrated TDN with a CD63 aptamer for the identification of exosomes [92] (Fig. 8E). The biosensor was coated with polydopamine (PDA), a semiconducting material for signal amplification. The presence of exosomes facilitated the formation of a TDN-aptamer-exosome complex. Under the catalysis of HRP, the biosensing platform generated enhanced PDA signals for the exosomes. Consequently, the biosensor was capable of quantifying A549-derived exosomes at the single-molecule level.

Certain proteins, including nucleolin, EpCAM, and MUC1, are specifically localized on the membranes of cancer cells. TDN-based cytosensors can effectively detect cancer cells by integrating aptamers as recognition elements [93–97] (Table 7). Various techniques, including fluorescent, electrochemical, and microfluidic technologies, have been employed for the identification of cancer cells. Fluorescent technology based on TDN has been developed for the detection of cancer cells. Unlike traditional dyes, semiconductor quantum dots (QDs) provide superior brightness and high quantum yields, making them ideal for efficient signal amplification. Wang et al. [98] proposed a 3D multipedal DNA walker (Fig. 9A), in which TDN was functionalized with the AS1411 aptamer to enable the precise recognition of HeLa cells. Upon encountering HeLa cells, the TDN interacted with nucleolin present on the cell membrane surface, leading to the dissociation of AS1411 from the capture probe. Subsequently, bipedal fuel DNA hybridized with the TDN, exposing two catalytic regions and forming a walker probe. As the TDN rolled along polystyrene microspheres (PS), the walker probe achieved autonomous multipedal motion. This innovative walking mechanism facilitated signal amplification through the fluorescence recovery of CdTe QDs located on the PS surface.

To achieve efficient cancer cell recognition, Chen et al. [99] proposed a dual-aptamer electrochemical strategy based on TDN and MOFs for the identification of MCF-7 cells (Fig. 9B). In this approach, TDN was combined with dual aptamers (AS1411 and MUC1). The novel MOFs (PCN-224) were used as nanocarriers for the cytosensor. The MOFs/HRP/Aptamer/Hemin nanoprobe served both as a recognition element and a signal tag. When MCF-7 cells were present, a TDN/cell/nanoprobe structure was formed on the electrode. Thereby, an enhanced electrochemical signal was produced through the catalysis of hydroquinone oxidation. This electrochemical cytosensor provided a significant diagnostic technique for MCF-7 cell analysis with a LOD of 6 cells/mL.

The microfluidic chip has emerged as a promising platform for capturing tumor cells due to its advantages, including high throughput and automated operation. Mi et al. [100] developed a microfluidic system that leveraged TDNs and aptamer-induced HCR for the efficient capture of MCF-7 cells (Fig. 9C). In this system, TDNs served as scaffolds on the chip. When MCF-7 cells were present, they specifically recognized and bound to the aptamer-HCR products. The apt-HCR/MCF-7 cell complexes were subsequently hybridized with the TDN scaffolds. The nuclease was applied to specifically cleaved TDN/apt-HCR structures, allowing the release of MCF-7 cells without causing damage. This microfluidic chip demonstrated high efficiency in both capturing and releasing MCF-7 cells from whole blood samples. This research underscores the broad application potential of microfluidic chips for tumor liquid biopsy, offering a valuable tool for cancer diagnostics and research.

2.2.3. Specific recognition sites based approaches

Multiple enzymes in cells maintain homeostatic balance, and

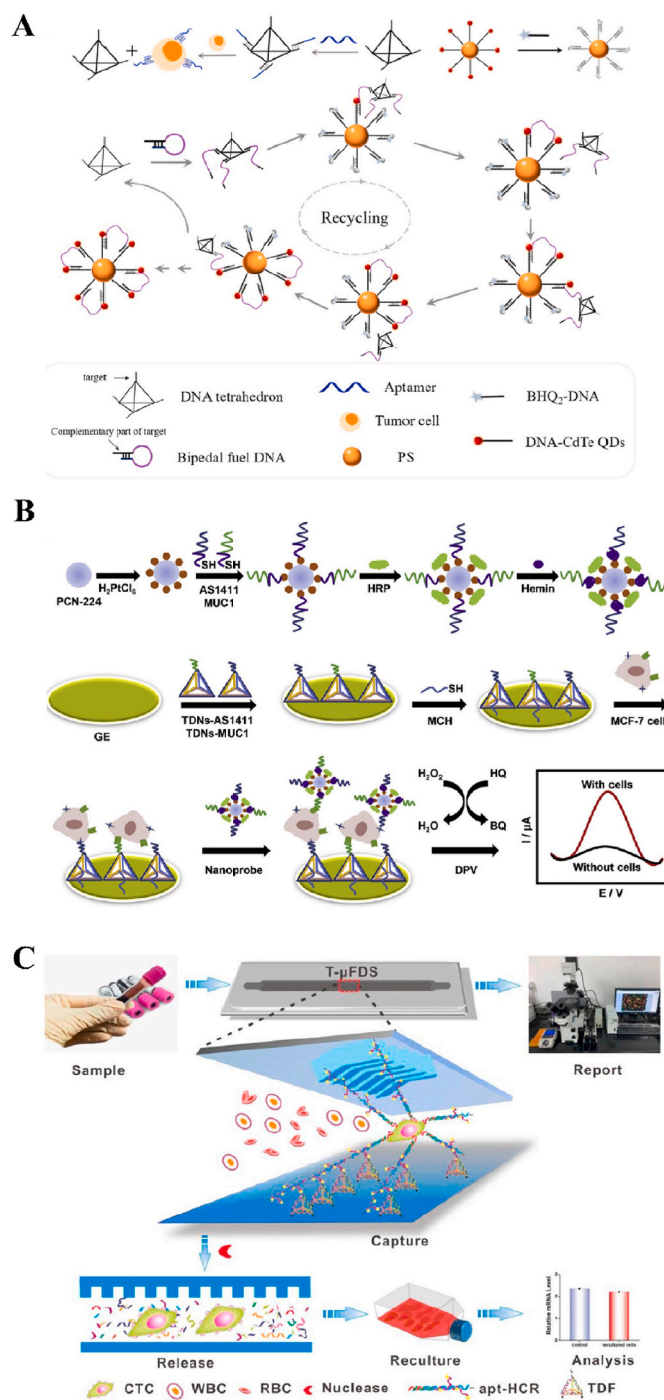


Fig. 9. Schematic illustration of TDN cytosensor for cancer cell identification. (A) A fluorescent strategy based on 3D multipedal DNA walker for HeLa cells identification. Reprinted from Ref. [98]. Copyright 2022, Elsevier. (B) A dual-aptamer electrochemical strategy integrating MOFs with TDN for the detection of MCF-7 cells. Reprinted from Ref. [99]. Copyright 2019, Elsevier. (C) TDNs and aptamer-induced HCR based microfluidic chip for the efficient capture and release of MCF-7 cells. Reprinted from Ref. [100]. Copyright 2022, Elsevier.

dysregulated enzyme expression is linked to cancers; for instance, telomerase is upregulated in more than 90 % of tumor cells [101]. Monitoring enzyme expression levels in vivo has emerged as a vital component of cancer diagnosis and medical research [102]. The combination of DNA nanomaterials with fluorescent techniques has advanced the mapping of intracellular biomarkers [103]. TDN has

become an ideal tool for enzyme assays because of the merits, such as efficient cellular internalization and numerous modification sites [104]. A widely adopted strategy for constructing enzyme biosensors involves modifying TDN with specific recognition sites tailored to the distinct characteristics of each enzyme.

Given the potential of DNA methyltransferase (DNA MTase) as a target for anticancer therapy, a fluorescence biosensing approach based on TDN was developed for sensitive DNA-adenine-methyltransferase (Dam MTase) detection [105] (Fig. 10A). The two edges of the TDN were modified with recognition sites for Dam MTase. Initially, the TDN was in a "signal off" state due to the close proximity of the fluorophores

and quenchers. When Dam MTase was present, it methylated the adenosine residues with the help of S-adenosyl methionine (SAM). In the presence of the restriction endonuclease *DpnI*, the TDN structure collapsed. This resulted in the release of fluorescent dyes and thereby switching the TDN to a "signal on" state. This biosensor achieved a LOD of 0.045 U/mL and was successfully applied for screening methylation inhibitors.

DNA repair enzymes, such as human apurinic/apyrimidinic endonuclease 1 (APE1) and 8-oxoguanine DNA glycosylase (8-oxoG DNA glycosylase), are fundamentally important for genetic integrity, with abnormal expression linked to various cancers [106]. TDN nanoprobe

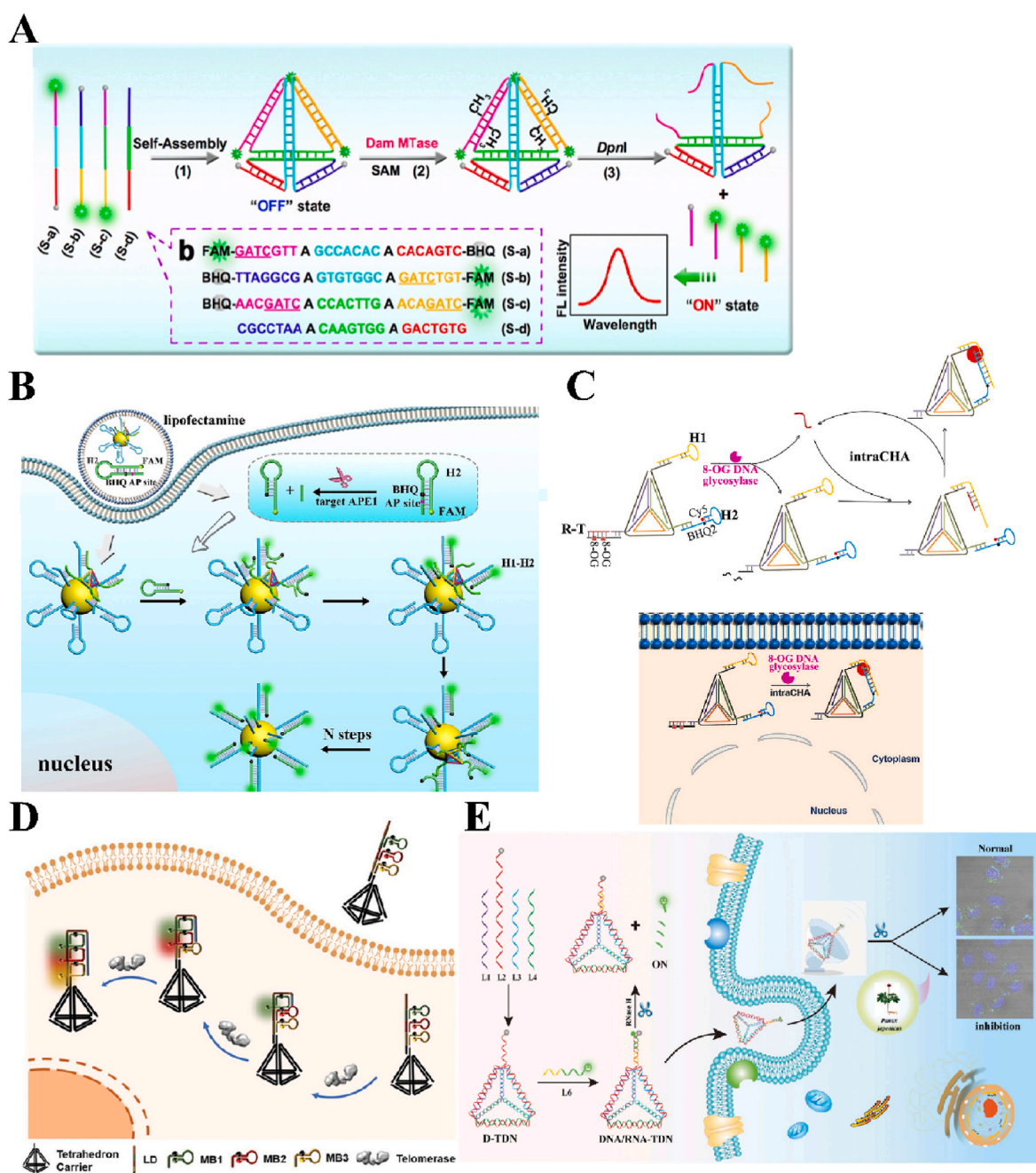


Fig. 10. Schematic illustration of TDN nanoprobe for intracellular enzymes imaging. (A) A fluorescent method based on collapse of TDN for "off-on" Dam MTase detection. Reprinted from Ref. [105]. Copyright 2017, American Chemical Society. (B) A fast-walking TDN walker for intracellular imaging of APE1. Reprinted from Ref. [107]. Copyright 2022, American Chemical Society. (C) CHA-TDN assisted nanoprobe for amplified intracellular imaging of 8-oxoG DNA glycosylase. Reprinted from Ref. [109]. Copyright 2023, Elsevier. (D) A lighting-up multicolor probe based on TDN for intracellular telomerase analysis. Reprinted from Ref. [111]. Copyright 2021, Royal Society of Chemistry. (E) A radar-like biosensor for natural compounds screening and RNase H imaging. Reprinted from Ref. [113]. Copyright 2021, Royal Society of Chemistry.

demonstrated significant potential as a promising tool for evaluating enzyme activity and screening drugs. Recently, dynamic functional DNA materials, such as DNA walkers, have emerged as promising molecular devices in the field of biosensing. Chai et al. innovatively proposed a four-armed 3D walker based on TDN for APE1 imaging [107] (Fig. 10B). The introduction of the TDN framework significantly enhanced the walking efficiency and nuclease resistance of the walker. The TDN with four arms hybridized with hairpins H1 modified on gold nanoparticles. Once entering the cells, the H2 hairpin, labeled with an AP site, FAM, and BHQ1, was recognized and cleaved by APE1, exposing the toehold area. Subsequently, H2 with an exposed toehold completely hybridized with H1, rapidly propelling the TDN. Meanwhile, the formation of the H1-H2 complex separated FAM from the quencher BHQ1, generating a fluorescence signal and enabling the imaging of APE1. Remarkably, the initial rate of the 3D TDN walker demonstrated a 4.54-fold increase compared to the free DNA walker, highlighting the potential of DNA walkers for efficient enzyme assays. Additionally, TDN can function as both an imaging and regulatory tool for cellular APE1 [108]. The specially designed TDN bound efficiently to APE1, inhibiting its activity with a half-maximal inhibitory concentration of 14.8 nM. The 8-oxoG DNA glycosylase was detected by combining an CHA and TDN-mediated sensing probe [109] (Fig. 10C). The TDN was integrated with a DNA strand (modified with 8-oxoG sites and a trigger strand), and two hairpin structures containing fluorophores. Endogenous 8-oxoG DNA glycosylase effectively recognized the 8-oxoG sites, enabling the release of the trigger strand. Later, intra-CHA reaction was initiated to produce a fluorescent signal. Compared to free CHA, this nano-system exhibited superior cell permeability for intracellular imaging of 8-oxoG DNA glycosylase.

Telomerase, consisting of telomerase RNA and reverse transcriptase, adds telomere repeat sequences (TTAGGG)_n to telomeres [110]. Its overexpression in most cancers is associated with unlimited cell proliferation, highlighting the importance of telomerase detection for cancer diagnostics and therapies. Xu's research team developed a multicolor probe for intracellular telomerase analysis [111] (Fig. 10D). This innovative probe involved the hybridization of a TDN with a DNA strand (LD). The LD contained specialized regions for three molecular beacons (MBs) and a telomerase substrate (TS). Under the action of telomerase, the TS domain produced repeats of the TTAGGG sequence. As the number of repeat units increased, the fluorophores of all three MBs were restored, yielding a pronounced fluorescent signal. Besides fluorophores, silver nanoclusters (AgNCs) were used in a TDN-supported biosensing platform [112]. TDN was enriched with cytosine-rich DNA probes, and telomerase introduced a single-strand TTAGGG extension, activating AgNC fluorescence through proximity to guanine-rich sequences. This method achieved highly sensitive telomerase quantification with a low LOD of 1 cell, effectively distinguishing healthy individuals from cancer patients.

Ribonuclease H (RNase H) is crucial in the HIV-1 reverse transcriptase pathway, and inhibiting its activity can disrupt viral replication, making RNase H inhibitors potential therapeutic agents against HIV/AIDS. Wang et al. [113] developed a radar-like nanostructure for screening natural compounds targeting RNase H and imaging RNase H (Fig. 10E). In this system, TDN was linked to a quencher-labeled long strand. In the absence of RNase H, a fluorophore-labeled RNA strand was hybridized with the long strand, resulting the quenched fluorescence. The presence of RNase H led to hydrolysis of the RNA chain, enabling the recovery of fluorescence signal. This radar-like monitor exhibited a LOD of 0.01 U/mL for RNase H. And three RNase H inhibitors were identified from 35 compounds of *Panax japonicus*. More information on TDN biosensing systems for detecting the different enzymes is briefly listed in Table 7 [114–118].

2.3. Metal ion detection

Heavy metal ions are identified as contaminants threatening human

health and environmental safety. Various spectrometry technologies, such as atomic absorption spectrometry and inductively coupled plasma mass spectrometry, have been employed for the effective analysis of metal ions [119]. Nevertheless, these current methodologies demand expensive equipment and specialized expertise, posing challenges for the rapid monitoring of these pollutants. Thus, there is an urgent need to develop a robust and accessible platform for sensing metal ions. Owing to their highly specific recognition abilities, DNAzyme-based biosensors present an ideal alternative for metal ion detection [120]. When integrated with TDN, metal-dependent DNAzymes can be shielded from nucleic acid degradation and interference from other ions. Herein, a DNAzyme-based electrochemical sensor was developed for Pb²⁺ detection [121]. The DNAzyme was precisely designed at one edge of the TDN. Upon the presence of Pb²⁺, the DNAzyme was activated to cleave the substrate, releasing the electrochemical group (methylene blue) on the electrode to produce a signal. This TDN sensor facilitated the detection of Pb²⁺ in tap and river water. In another study, a Pb²⁺-sensitive DNAzyme/cleavage duplex was assembled at one vertex of TDN [122] (Fig. 11A). With the assistance of Pb²⁺, the active DNAzyme cleaved the substrate, generating a fluorescent signal from FAM release. This sensor exhibited enhanced nuclease resistance compared to free DNAzymes in human serum. Signal amplification strategies, including HCR and CHA, have been utilized to enhance the sensitivity and speed of metal ion detection. Zhang et al. [123] introduced an electrochemical sensing platform for detecting serum copper (Cu²⁺) by integrating TDN with CHA and HCR. In this setup, TDN acted as a scaffold to minimize nonspecific binding. The use of magnetic beads facilitated the extraction of targets from complex samples and reduced background signals. This platform achieved a LOD of 0.33 fM for Cu²⁺. In addition to electrochemical methods, the fluorescent sensing strategy has been employed for metal ion assays. Kong et al. developed a tetrahedral sensing platform based on hyper-branched HCR (hHCR) for Pb²⁺ detection [124]. The absence of Pb²⁺ initiated the TDN-hHCR aggregation, resulting in an amplified FRET signal. By combining TDN with HCR, the controllability of HCR was improved, significantly accelerating its reaction kinetics. This fluorescent biosensor enabled rapid detection of Pb²⁺ within 20 min and was successfully applied for accurate detection in real samples, including river water, fruits, vegetables, and grains. In addition to metal ion-dependent DNAzymes, aptamers provide an alternative approach for metal ion recognition. Chen et al. developed a colorimetric paper chip for mercury ion (Hg²⁺) analysis, valued for its simplicity, visual clarity, and user-friendliness [125] (Fig. 11B). In this design, TDN served as a platform for anchoring aptamers to enhance target capture efficiency. In the presence of Hg²⁺, the aptamer bound to the ion, causing it to detach from the TDN. As a result, streptavidin-labeled HRP cannot bind to the TDN. Upon adding the TMB-H₂O₂ solution, a reduced color intensity was observed in the detection zone, enabling visual monitoring of Hg²⁺. This paper chip also holds the potential for detecting other targets by simply changing the aptamers.

2.4. Mycotoxins and small molecule detection

Small molecules, typically under 1000 Da, include therapeutic agents, mycotoxins and metabolic compounds essential for biological functions. Monitoring of these small molecules in animal-derived foods and agricultural products is vital for ensuring food safety. Recent concerns about antibiotic residues and mycotoxins in agriculture have spurred research into various detection methods, including fluorescent and electrochemical biosensing platforms [126]. Various nanomaterials, like MBs, AuNPs, Fe₃O₄NPs, and rGO, endow with the merits of high specific surface area and excellent electrical conductivity, making them the ideal materials for TDN-based biosensor construction. Herein, aptamers are often used as target recognition elements for agents and mycotoxins. In one study, Cai et al. [127] developed a fluorescent biosensor based on magnetic beads (MBs) and TDN for detecting tetracycline (TET). The aptamer was modified to TDN to capture TET, while

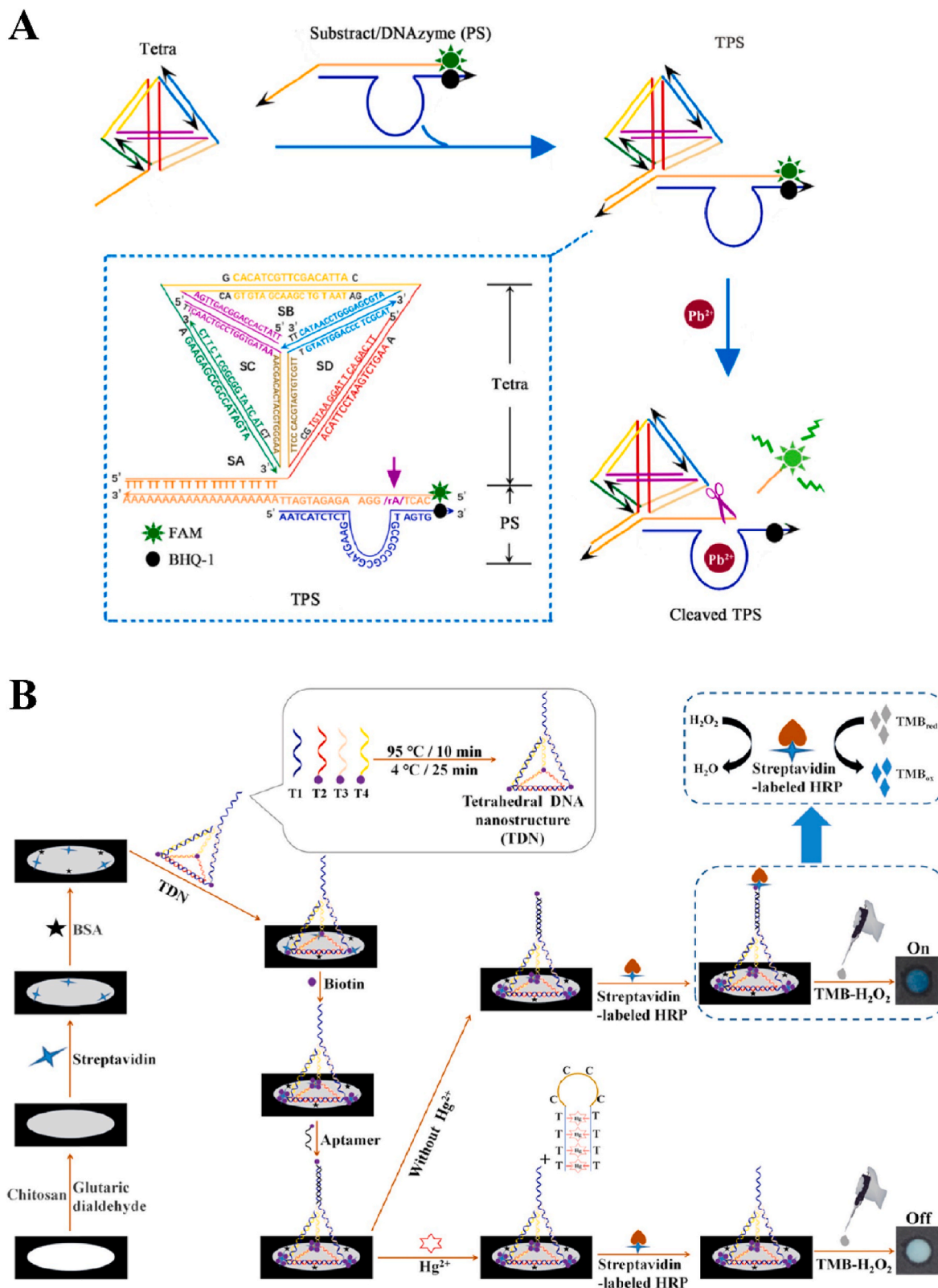


Fig. 11. Schematic illustration of TDN aptasensors for metal ions detection. (A) Pb^{2+} -sensitive DNAzyme based on TDN for the analysis of Pb^{2+} . Reprinted from Ref. [122]. Copyright 2021, Elsevier. (B) TDN-functionalized colorimetric paper for Hg^{2+} visual monitoring. Reprinted from Ref. [125]. Copyright 2022, Elsevier.

MBs provided a large surface area for TDN loading. The presence of TET triggered the release of the primer strand, which subsequently initiated RCA for signal enhancement. This probe enabled the quantification of TET in fish and honey samples (Fig. 12A). Similarly, another fluorescent

method combining AuNPs and TDNs was established for detecting Ochratoxin A (OTA) in corn, effectively preventing aptamer crowding [128]. In both of these examples, the use of MBs and AuNPs served as signal amplifiers by providing a large surface area for TDNs. The

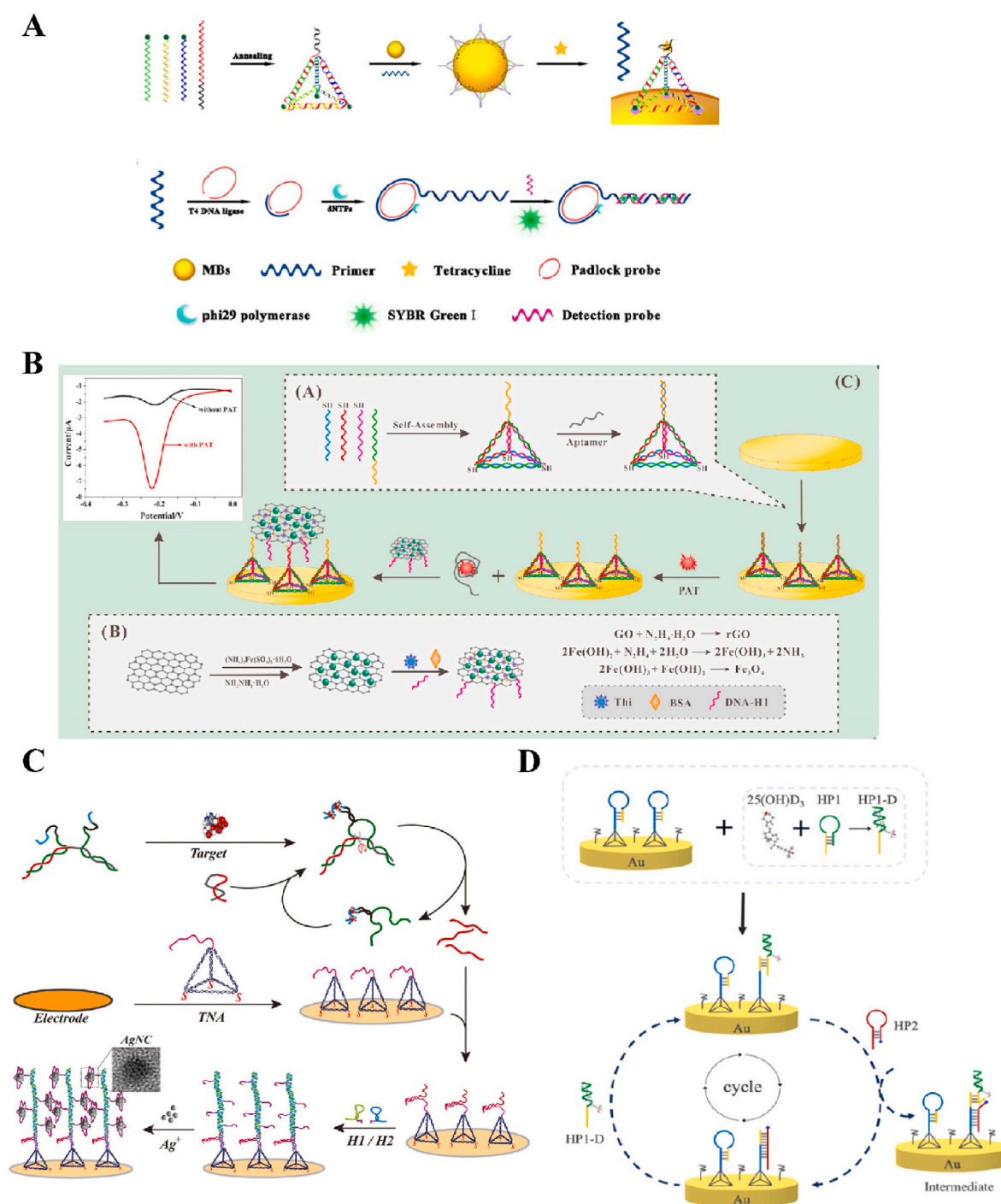


Fig. 12. Schematic illustration of TDN aptasensors for mycotoxins and small molecules detection. (A) A fluorescent TDN aptasensor based on MBs and RCA for TET detection. Reprinted from Ref. [127]. Copyright 2021, American Chemical Society. (B) A TDN-based electrochemical biosensing platform based on Fe₃O₄NPs/rGO nanocomposite for the detection of patulin. Reprinted from Ref. [129]. Copyright 2020, Elsevier. (C) An ECL biosensor based on the HCR and DNA-templated silver nanoclusters for amplified detecting ATP. Reprinted from Ref. [133]. Copyright 2022, Elsevier. (D) An electrochemical strategy involving CHA and TDN for the amplified assay of 25(OH)D₃. Reprinted from Ref. [135]. Copyright 2021, Elsevier.

integration of nanomaterials with TDN also enhanced the amplified electrochemical sensing of agents and mycotoxins. He et al. [129] innovatively developed a TDN-based electrochemical biosensor based on Fe₃O₄NPs and rGO for the detection of patulin (PAT) (Fig. 12B). Fe₃O₄NPs are recognized as effective electrochemical catalysts, while rGO serves as an ideal substrate material that improves the dispersion of Fe₃O₄NPs. Therefore, the combination of Fe₃O₄NPs and rGO synergistically enhanced the electrochemical signal. TDNs were integrated with an aptamer for the effective binding of PAT. When PAT is present, the

aptamer bound to it and was subsequently released from the TDN. Meanwhile, Thi-labeled Fe₃O₄NPs/rGO nanocomposites can integrate with TDNs, resulting in an increased Thi current signal. This aptasensor achieved a LOD of 30.4 fg/mL for PAT and was successfully applied to detect PAT in apple juice samples. AuNPs also facilitated the detection of theophylline in serum, generating significant electrochemical responses [130].

Abnormal levels of small molecules like adenosine, adenosine triphosphate (ATP), and vitamin D are related to diseases including

Alzheimer's, Parkinson's, and skeletal disorders. Adenosine influences various cellular functions, including neuronal activity and vascular function. Researchers have advanced a range of TDN aptasensors utilizing techniques such as electrochemistry, fluorescence, and ECL. By integrating aptamers with DNAzymes, they have enhanced the amplification efficiency for analyzing adenosine and ATP. In one study, an electrochemical biosensor, incorporating AuNPs and TDN, was developed specifically for the detection of adenosine [131]. AuNPs acted as rolling motors, enhanced with polyadenine blocks, rA sites, and ferrocene tags. An aptamer-regulated DNAzyme (aptazyme) connected the TDN to the rolling motor. When adenosine is present, the aptazyme activated and cleaved the rA site, releasing ferrocene for electrochemical signaling. The biosensor performed a LOD of 0.17 nM for rapid adenosine sensing. Chang's group developed another electrochemical biosensor using a configuration-switchable TDN and G-quadruplex for ATP detection, a key energy substrate in biological processes [132]. The aptamer at the TDN's edge reconfigured upon ATP presence, forming a G-quadruplex and producing a dynamic electrochemical response with a LOD of 50 pM. The ECL biosensing platform demonstrated outstanding analytical performance for ATP detection. In a separate study, an ECL biosensor utilizing HCR and TDN was designed to achieve amplified detection of ATP [133] (Fig. 12C). The aptazyme recognized ATP and regulated DNAzyme activity, inducing HCR and forming long double-stranded DNA on the electrode. These pre-programmed double-stranded DNA sequences, rich in cytosine, were synthesized with silver nanoclusters for ECL signal amplification with a limit detection of 38.2 fM for ATP. This ECL biosensor was also adapted for quinine detection by using a quinine aptamer. Real-time monitoring of ATP is crucial for unveiling the dynamic changes within intracellular ATP, thereby aiding in the diagnosis of related diseases. Researchers developed a fluorescent biosensor utilizing TDN for imaging intracellular ATP [134]. The TDN acted as both an aptamer module and a carrier for fluorescent dyes, amplifying signals upon ATP interaction. This system differentiated between tumor cells and normal cells according to ATP levels.

25-Hydroxyvitamin D₃ (25(OH)D₃) serves as a crucial biomarker for evaluating vitamin D levels in the human body. A CHA-TDN was proposed for 25(OH)D₃ determination [135] (Fig. 12D). In this approach, TDN was anchored on the electrode surface, allowing for the assembly of a hairpin aptamer/25(OH)D₃ complex (HP1-D). This complex could then be displaced by HP₂ hairpin, triggering CHA cycles. The sensor was effectively used for serum 25(OH)D₃ evaluation, highlighting its potential in diagnosing vitamin D deficiency. The aforementioned TDN aptasensors for metal ion and other molecule detection are summarized in Table 8.

Table 8
FTDN-based biosensors for metal ion and chemical compound detection.

Target	Method	Signal labeling	Detection Range	LOD	Publish year	Ref.
Lead ions	Fluorescence	FAM	10 to 100 nM	0.9125 nM	2022	[119]
Lead ions	Electrochemical	Methylene blue	0.01 to 100 μM	0.01 μM	2019	[121]
Lead ions	Fluorescence	FAM	1 nM to 1000 nM	1 nM	2021	[122]
Lead ions	Fluorescence	Cy3 and Cy5	0 to 100 nM	0.25 pM	2021	[124]
Serum copper	Electrochemical	Methylene blue	0.001 to 2000 pM	0.33 fM	2021	[123]
Mercury detection	Colorimetric	TMB/HRP	0.1 pM to 100 nM	30 fM	2022	[125]
Tetracycline	Fluorescence	6-carboxy-X-rhodamine	0.01 to 50 ng/mL	0.006 ng/mL	2020	[126]
Tetracycline	Fluorescence	SYBR Green I	0.001 to 10 ng/mL	0.724 pg/mL	2021	[127]
Ochratoxin A	Fluorescence	Cy5	0.01 to 10 ng/mL	0.005 ng/mL	2022	[128]
Patulin	Electrochemical	Fe ₃ O ₄ NPs/rGO	0.5 μg/mL to 50 ng/mL	30.4 fg/mL	2020	[129]
Theophylline	Electrochemical	Methylene blue	0.1 μM to 500 μM	0.07 mM	2018	[130]
Adenosine	Electrochemical	AuNPs	0.5 to 1500 nM	0.17 nM	2020	[131]
ATP	Electrochemical	G-quadruplex-Hemin	0.1 nM to 1 μM	50 pM	2020	[132]
ATP	Fluorescence	FAM and BHQ1	1 pM to 10 nM	0.40 pM	2023	[134]
ATP and quinine	ECL	AgNC	0 to 100 nM/0 to 10 nM	38.2 fM/3.7 pM	2022	[133]
25-hydroxyvitamin D ₃	Electrochemical	Au	0.1 nM to 1 μM	0.026 nM	2022	[135]

2.5. Multiple biomarkers detection

The development and progression of diseases are often associated with multiple biomarkers. However, to date, DNA biosensors have primarily been utilized for single biomarker detection due to their limited capacity for multi-target assays [136]. Owing to the abundant modification sites of TDN, it allows for the integration of various nucleic acid probes and functional units, thereby enhancing detection efficiency [137–140]. Consequently, numerous TDN-based biosensing platforms have been developed for the simultaneous detection of nucleic acids, proteins, and enzymes associated with cancer, paving the way for more precise diagnostic approaches (Table 9). Due to the low intracellular levels of nucleic acid markers, signal amplification strategies such as HCR and CHA are utilized in TDN-based biosensing platforms to enable sensitive miRNA quantification [141]. For instance, 3D HCR based on TDN enabled the synchronous imaging of miRNA-21 and miRNA-203 in living cells [142] (Fig. 13A). The TDN was designed with four HCR probes positioned at its four vertices. Upon entering cancer cells, the overexpressed miRNA-21 and miRNA-203 triggered two HCR amplification reactions, leading to the formation of the 3D TDN assembly. This process, characterized by the separation of the fluorophore and quencher, generated significant fluorescent signals. Consequently, this nanoprobe achieved enhanced sensitivity for detecting miRNAs down to pM levels, while also enabling dual-color imaging. Simultaneous real-time detection of enzymes and nucleic acid biomarker is essential for tumor cell identification [143]. Zhang's team developed a 3D DNA nanofirework incorporating of double TDNs for the simultaneous imaging of miRNA-21 and telomerase [144] (Fig. 13B). These TDN probes could enter cells via endocytosis. miRNA-21 was captured by DNA strands on two vertices of the P-TDN, generating a Cy3 fluorescent signal as the quencher was released. Meanwhile, the presence of telomerase led to the recovery of a Cy5 fluorescent signal. With the introduction of the T-TDN, a self-assembled 3D DNA superstructure was formed through a strand displacement reaction, significantly amplifying the dual biomarker signals. This innovation enabled accurate in situ differentiation between non-tumorous and malignant cells.

Many cancer biomarkers have distinct spatial locations within tumor cells, such as glycoproteins on the membrane and nucleic acids in the cytoplasm [145], necessitating multiplexed monitoring for accurate information on cell types and cancer progression. The integration of aptamers and TDNs facilitated precise identification of cancer cells [146, 147]. Recently, Dai et al. [148] designed an innovative logic nanodevice combining TDNs and DNAzymes for simultaneous imaging of nucleolin and miRNA-21 (Fig. 13C). The TDN was functionalized with a linker-blocker-DNAzyme-substrate unit, where the blocker strand served to prevent false-positive signals. The AS1411 aptamer was pre-anchored to nucleolin proteins on the cancer cell membrane.

Table 9
FTDN-based biosensors for simultaneous detection of multiple biomarkers.

Target	Method	Signal labeling	Detection Range	LOD	Living cells	Publish year	Ref.
miRNA-21/miRNA-155	Electrochemical	Fc and MB	0.1 fM to 10 nM	18.9 aM and 39.6 aM	/	2020	[140]
miRNA-217/miRNA-196a	Fluorescent	FAM and Cy5	0.1 pM to 1 nM	21 fM/32 fM	HPNE/BxPC-3 cells	2023	[141]
miRNA-21/miRNA-203	Fluorescent	FAM and Cy3	0.1 to 200 nM	1.4 pM and 2.0 pM	MCF-7/MCF-10A cells	2023	[142]
Telomerase/miRNA-21	Fluorescent	Cy3 and Cy5	0 to 16000 cell/ μ L and 0 to 100 nM	34 pM/100 cells/ μ L	HeLa/HepG2/MCF-7/MCF-10A/MCR-5 cells	2023	[144]
MUC1/miRNA-21	Fluorescent	Cy3 and Cy5	0 to 400 nM/0 to 200 nM	201 pM/28.3 pM	MCF-7/HeLa/HepG2/L02 cells	2022	[146]
miRNA-21/miRNA-155	Fluorescent	Cy3 and Cy5	0 to 50 nM/0 to 100 nM	26 pM/85 pM	MDA-MB-231/MCF-7/A549/L02 cells	2022	[147]
Nucleolin/miRNA-21	Fluorescent	Cy5	100 nM/0 to 100 nM	0.81 nM (miRNA-21)	MCF-7/MCF-10A cells	2023	[148]
miR-let-7a/miR-375/miR-21	Electrochemical	Au	0.2 to 500 fM/0.01 to 700 pM/0.04 to 100 nM	0.2 fM/10 fM/40 pM	/	2020	[150]
Myc/TK1/GalNAc-T mRNA	Fluorescent	FAM, Cy3 and Cy5	10 nM to 150 nM	3.1 nM/1.2 nM/3.2 nM	MCF-7/MCF-10A cells	2017	[151]
miRNA-21/miRNA-221/miRNA-155	Fluorescent	FAM, ROX and Cy5	/	1 nM	MCF-7/HepG2/MCF-10A cells	2020	[152]
miRNA-21/miRNA-122/miRNA 223	Fluorescent	Cy3, Cy3.5 and Cy5	0.2 to 10 nM	/	/	2020	[153]
MUC1/EpCAM/PTK7	Fluorescent	FAM, TAMRA, Cy5	/	/	HeLa/MCF-7/MDA-MB-468 cells	2024	[154]
HPV-16/HPV-18/HPV-52	ICP-MS	Au NPs/Ag NPs/Pt NPs	0.1 pM to 50 pM	0.218 pM/ 0.491 pM/0.268 pM	/	2023	[156]

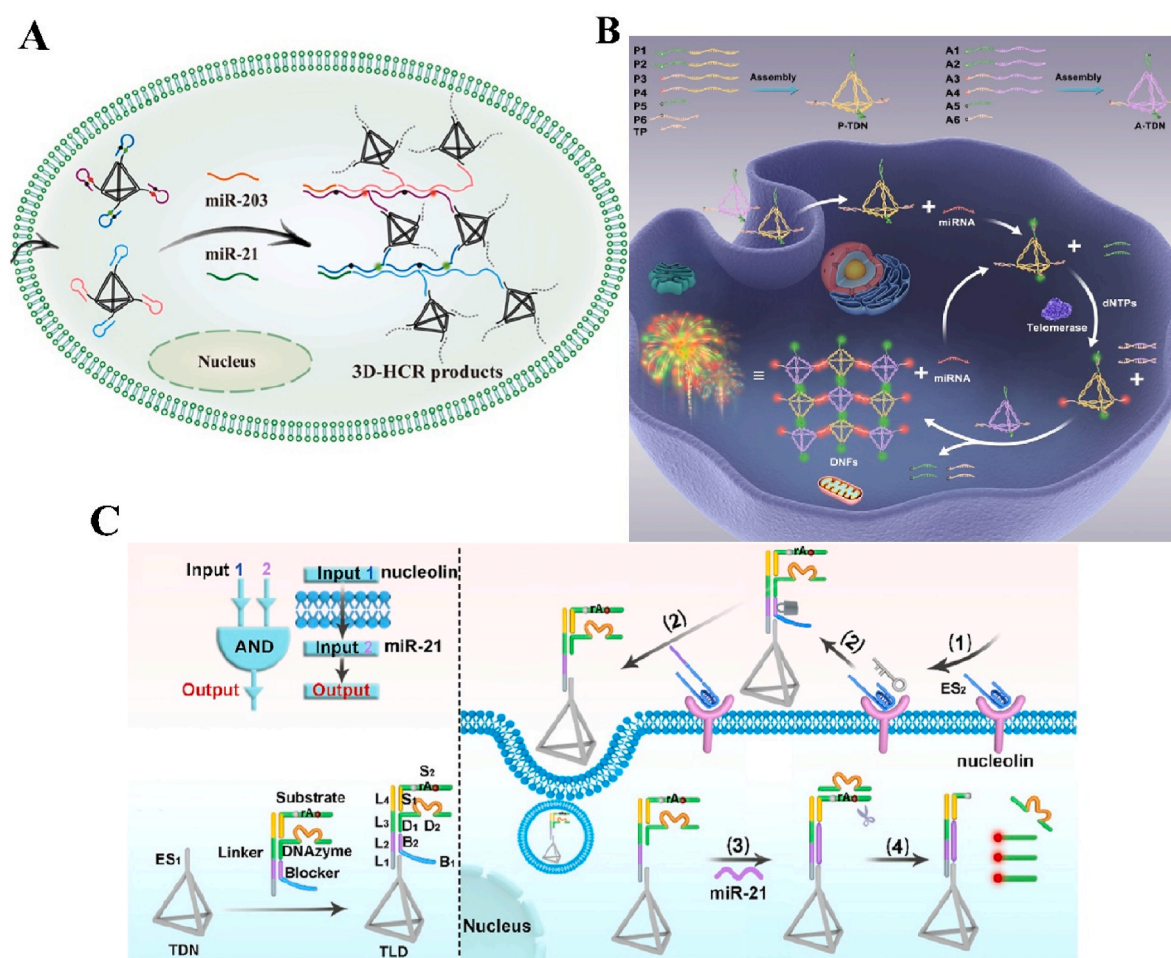


Fig. 13. Schematic illustration of TDN-based fluorescent biosensors for duplex biomarkers detection. (A) 3D HCR-based TDN for simultaneous monitoring of miRNA-21 and miRNA-203. Reprinted from Ref. [142]. Copyright 2022, Elsevier. (B) 3D DNA nanofirework involving double TDNs for simultaneous imaging of miRNA-21 and telomerase. Reprinted from Ref. [144]. Copyright 2023, American Chemical Society. (C) AND logic nanodevice integrating TDN with DNAzyme for imaging nucleolin and intracellular miRNA-21. Reprinted from Ref. [148]. Copyright 2023, American Chemical Society.

Initially, the TDN remained in a "signal-off" state due to the tight binding of the blocker strand. Upon encountering a cancer cell, the AS1411 aptamer (input 1) interacted with the blocker strand. Concurrently, miRNA-21 activated the DNAzyme-assisted reaction, leading to the generation of a fluorescent signal (input 2). This biosensing system achieved dual-biomarker detection, spanning from the cell membrane to the cytoplasm, offering a promising platform for the simultaneous detection of multiple biomarkers.

Except for dual detection strategies, TDN-based sensing platforms have also been employed for the simultaneous analysis of three biomarkers, including miRNA, cell membrane proteins, and HPV-DNA. This approach offers a promising solution for the precise identification of tumor cells and the accurate diagnosis of diseases [149–152]. For example, Chen et al. [153] developed a fluorescent biosensor based on TDNs for the simultaneous detection of miRNA-21, miRNA-122, and miRNA-223, which are overexpressed in the early stages of liver cancer (Fig. 14A). This TDN system was designed to incorporate three adaptor strands, with TOTO-1 serving as the fluorescence donor and fluorophore-functionalized strands (FRET strands) acting as receptors. In the presence of miRNA-21, miRNA-122, and miRNA-223, these target miRNAs hybridized with the FRET strands and adaptor strands positioned at the vertices of the TDN. Consequently, efficient FRET occurred between TOTO-1 and the three fluorophores. The biosensor demonstrated effective multiplex detection in 10 % human serum, providing valuable assistance in liver cancer staging. In addition to cellular biomarkers detection, TDN-based aptasensors have also been utilized for

the detection and imaging of multiple cell membrane proteins. Ouyang et al. developed a logic gate TDN nanoplatfor for imaging three specific cell membrane glycoproteins: MUC1, EpCAM, and PTK7 [154] (Fig. 14B). The TDN was functionalized with three aptamers and streptavidin (SA). Initially, the fluorescence of each aptamer was quenched by complementary DNA oligos. Upon encountering cancer cells, the corresponding DNA oligos were removed from two aptamers, allowing SA to anchor the TDN to the cell membrane for internalization prevention. Subsequently, a second-order logic gate was activated, releasing the aptamers and restoring fluorescence. This logic gate-based system provided a multi-color sensing platform capable of distinguishing cancer cells from normal cells, facilitating the construction of a cell recognition library. The integration of quantitative single-molecule counting significantly enhanced the potential of this approach for the precise diagnosis of cancer cells.

Accurate quantification of HPV-DNA is critical for the diagnosis of cervical cancer [155]. Leveraging the CRISPR-Cas self-amplification strategy, Wu's team developed an innovative inductively coupled plasma mass spectrometry (ICP-MS) biosensor based on TDN and metal nanoparticle for the simultaneous detection of HPV-16, HPV-18, and HPV-52 [156] (Fig. 14C). The presence of the three target DNA sequences activated the trans-cleavage activity of the Cas12a/crRNA complex, leading to the release of short DNA fragments. These released DNA fragments were unable to anchor the metal-nanoparticle probes onto TDN-modified magnetic bead probes (TDN-MBs), resulting in a significant ICP-MS signal. This biosensor was successfully applied to

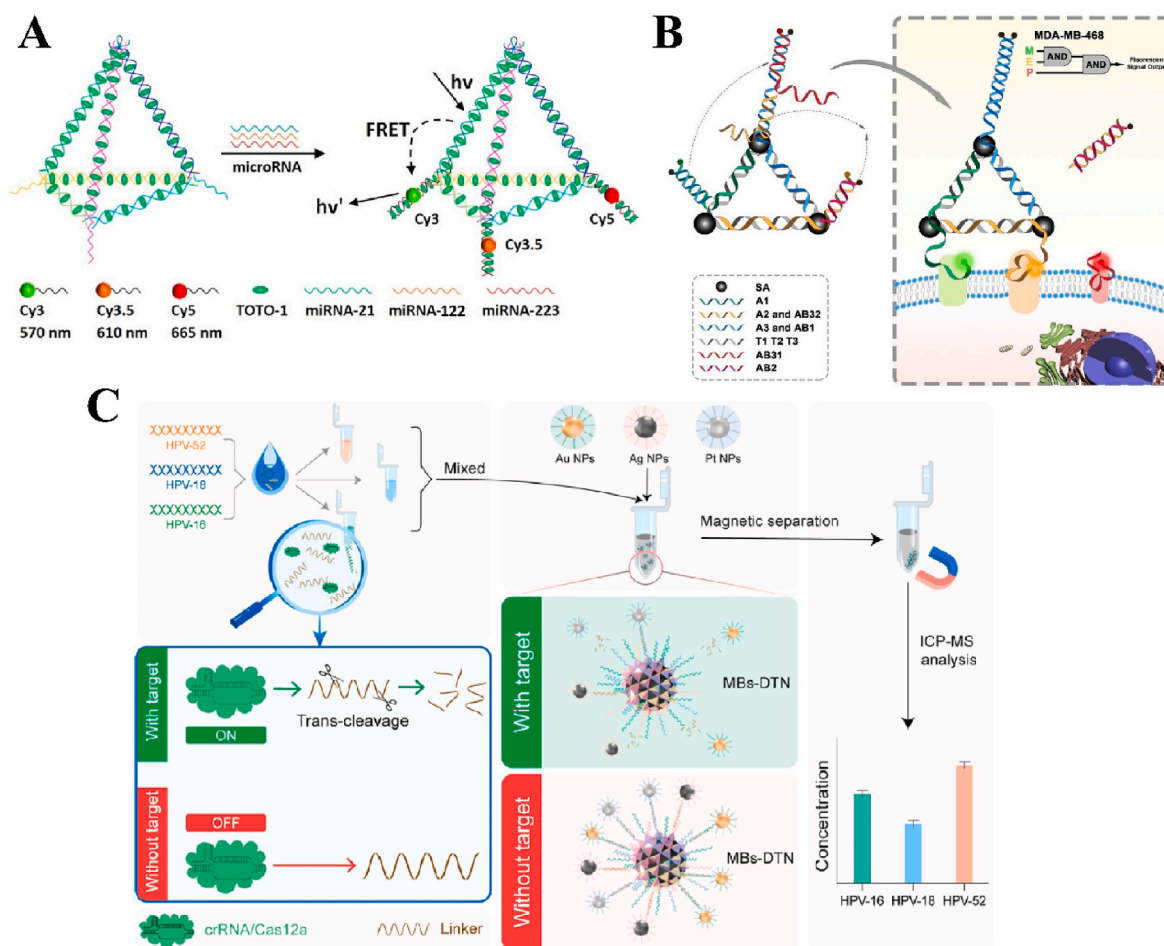


Fig. 14. Schematic illustration of TDN-based biosensing platforms for triple biomarkers detection. (A) TOTO-1 embedded TDN aptasensor for simultaneously miRNA-21, miRNA-122, and miRNA-223 detection. Reprinted from Ref. [153]. Copyright 2019, Elsevier. (B) A logic gate-based TDN nanoplatfor for the simultaneous imaging of MUC1, EpCAM, and PTK7 on cancer cell membrane. Reprinted from Ref. [154]. Copyright 2023, Elsevier. (C) An ICP-MS biosensor integrating TDN with CRISPR technology for the simultaneous detection of HPV-16, HPV-18, and HPV-52. Reprinted from Ref. [156]. Copyright 2023, Elsevier.

detect HPV-DNA in cervical swab samples. Notably, the TDN-MBs exhibited superior sensitivity for HPV-DNA compared to ssDNA-MBs, highlighting the potential of CRISPR-based technologies for the detection of multiple biomarkers.

3. Biosensing-treatment platforms

In recent years, theranostics has garnered significant attention in both research and clinical fields. Due to its unique structural and biomedical properties, TDN provides an excellent three-dimensional carrier for a variety of therapeutic agents, effectively bridging the gap between cancer diagnostics and drug delivery [157]. Wang et al. [158] developed a nano-theranostics platform utilizing TDN and AuNCs for tumor imaging and therapy (Fig. 15A). This system involved two sequential disassembly processes culminating in drug release. Upon entering tumor cells, legumain induced ligand hydrolysis on AuNCs, releasing the fluorophore Cy5 for cancer imaging. Subsequently, TDN collapse was triggered by GSH/TK1 mRNA, facilitating DOX release and gene silencing at the tumor site. The TDN/AuNCs nanocomplex notably enhanced stability and therapeutic efficacy against breast cancer compared to bare TDN. miRNAs are vital cancer biomarkers and therapeutic targets that play a significant role in cancer treatment. One study proposed a dual-miRNA-guided nanotheranostic system based on TDN [159] (Fig. 15B). The TDN was preloaded with the tumor suppressor miRNA-122. Upon entering hepatocellular carcinoma (HCC) cells, the oncogenic miRNA-155 induced an entropy-driven reaction, leading to TDN aggregate assembly for HCC imaging. Concurrently, miRNA-122 was released from TDN, synergistically suppressing HCC cells. This innovative platform demonstrated effective *in vivo* theranostics for HCC and could be adapted for broader theranostic applications by incorporating other nucleic acids.

4. Conclusions and prospects

DNA nanostructures-based biosensors are extensively applied in disease diagnosis, food safety, and environmental monitoring. This review emphasizes recent advancements in the FTDN biosensing platforms. According to our comprehensive illustration, FTDN-based biosensors serve as multifunctional sensing tools capable of detecting diverse biomarkers, encompassing nucleic acid, protein, mycotoxin, agents, and metal ion. Notably, TDN characterized by three vertices function as the fundamental components of the biosensing platform, enabling integration with various signal transduction modes, including fluorescence, electrochemical, ECL, and SERS, thereby facilitating the simultaneous determination of multiple biomarkers. This review demonstrates the innovative applications of advanced technologies and cutting-edge nanomaterials, such as CRISPR technology, metal nanoparticles, DNA walkers, MOFs, and rGO, in accelerating detection speed and improving sensitivity. Additionally, FTDN is recognized as an effective tool for monitoring tumor-associated biomarkers within living cells and even *in vivo* in consideration of its numerous advantages, such as excellent cell permeability and non-cytotoxic properties. Furthermore, TDN also serves as an efficient carrier for drug delivery, expanding its applications beyond diagnosis to therapeutic treatments.

FTDN-based biosensors have achieved significant advancements in multi-biomarker detection. However, several challenges remain to be addressed. (1) The structure of FTDN can be influenced by the complex components and interfering substances in some samples, which affects detection stability and limits its application in clinical sample bioassays. (2) FTDN-based fluorescent biosensors are widely applied in imaging intracellular biomarkers, such as miRNA, mRNA, and protein. However, these biosensors may encounter challenges, including false positive signals and an "always active" state. For instance, signals can be triggered by biomarkers before reaching the specific organelle within the cell. Therefore, the development of FTDN biosensors capable of precisely controlling biomarker imaging within cells is urgently needed. (3)

Most reported FTDN-based biosensors are designed for detecting a single metal ion or mycotoxin, which limits their broader application in environmental monitoring and food safety. Consequently, the development of novel FTDN-based biosensors with the capability to simultaneously detect multiple metal ions or mycotoxins is highly desirable. (4) The detection of multiple biomarkers requires the integration of additional probes. The design of FTDN plays a crucial role in achieving accurate and simultaneous detection. Factors such as the probe sequence and the size of the FTDN may significantly impact the efficiency of target signal conversion. Thus, systematic guidelines, such as TDN-based DNA computation, are urgently needed to improve the design and functionality of these biosensors. On the other hand, existing FTDN biosensors are typically designed for the simultaneous detection of multiple biomarkers of a single specific type. However, the progression of diseases is often associated with various biomarkers, such as RNA and proteins. Therefore, developing FTDN biosensing platforms capable of simultaneously detecting different types of biomarkers holds significant value for advancing precision medicine.

Fortunately, advancements in nanotechnology have continually driven progress in the development of DNA nanostructure probes, harnessing the exceptional robustness of FTDN. (1) Significant efforts have been made to prevent the nonspecific elimination of TDNs through chemical and physical modifications. For instance, TDNs coated with polyethyleneimine (PEI) demonstrated a prolonged metabolic duration *in vivo* compared to the unmodified TDN group [160]. Additionally, the incorporation of a nuclear localization signal (NLS) peptide onto the TDN vertex via click chemistry enhanced the lysosomal escape capability of TDNs, enabling effective biosensing in both the cytoplasm and the nucleus [161]. (2) Organelle-specific photoactivation biosensing strategy presents an excellent solution for avoiding the "always active" state. For instance, Li et al. [162] developed a photoactivatable engineered DNA sensor designed for APE1 imaging within intracellular organelles, including mitochondria and the nucleus. By utilizing deep-tissue penetrable NIR light as a trigger, this approach enabled spatially controlled monitoring of APE1 *in vivo*. Additionally, the incorporation of TPP and TAT peptides facilitated precise targeting of mitochondria and the nucleus. Therefore, the integration of photoactivation with organelle-specific targeting represents a promising strategy for the precise mapping of subcellular biomarkers *in vivo*. (3) To address the growing demand for environmental monitoring and food analysis, group-targeting aptamers have garnered significant attention from researchers. Unlike traditional aptamers, group-targeting aptamers have the unique ability to simultaneously identify multiple targets [163]. By integrating these multifunctional aptamers with TDN, the practicability of detecting metal ions and mycotoxins can be significantly enhanced. (4) Computer simulation techniques have become indispensable tools for predicting and simulating the reaction processes between probes and targets, greatly aiding in the design and optimization of FTDN. Molecular modeling is commonly employed to predict the bonding interactions between probes and targets, such as hydrophobic interactions [164]. Furthermore, molecular dynamics simulations enable the investigation of conformational changes during the interaction between FTDN and targets. It can facilitate the investigation of structural modifications and sequence variations to improve the functionality of TDN biosensors. For example, Su's group utilized simulation software to assess the distance between different fluorescent groups on TDN, effectively minimizing fluorophore crosstalk [165]. Overall, computer simulations offer a powerful approach to uncovering the underlying mechanisms of TDN-target interactions, which is essential for enhancing the selectivity and specificity of FTDN biosensors. (5) DNA classifiers have emerged as a significant advancement in the field of biosensing. Fan's group innovatively introduced a TDN-based DNA classifier for multidimensional molecular classification [166]. Unlike conventional analyses that rely on single-dimensional molecules, this TDN-based classifier enabled the integration and translation of multi-dimensional molecular information into a unified sensing signal.

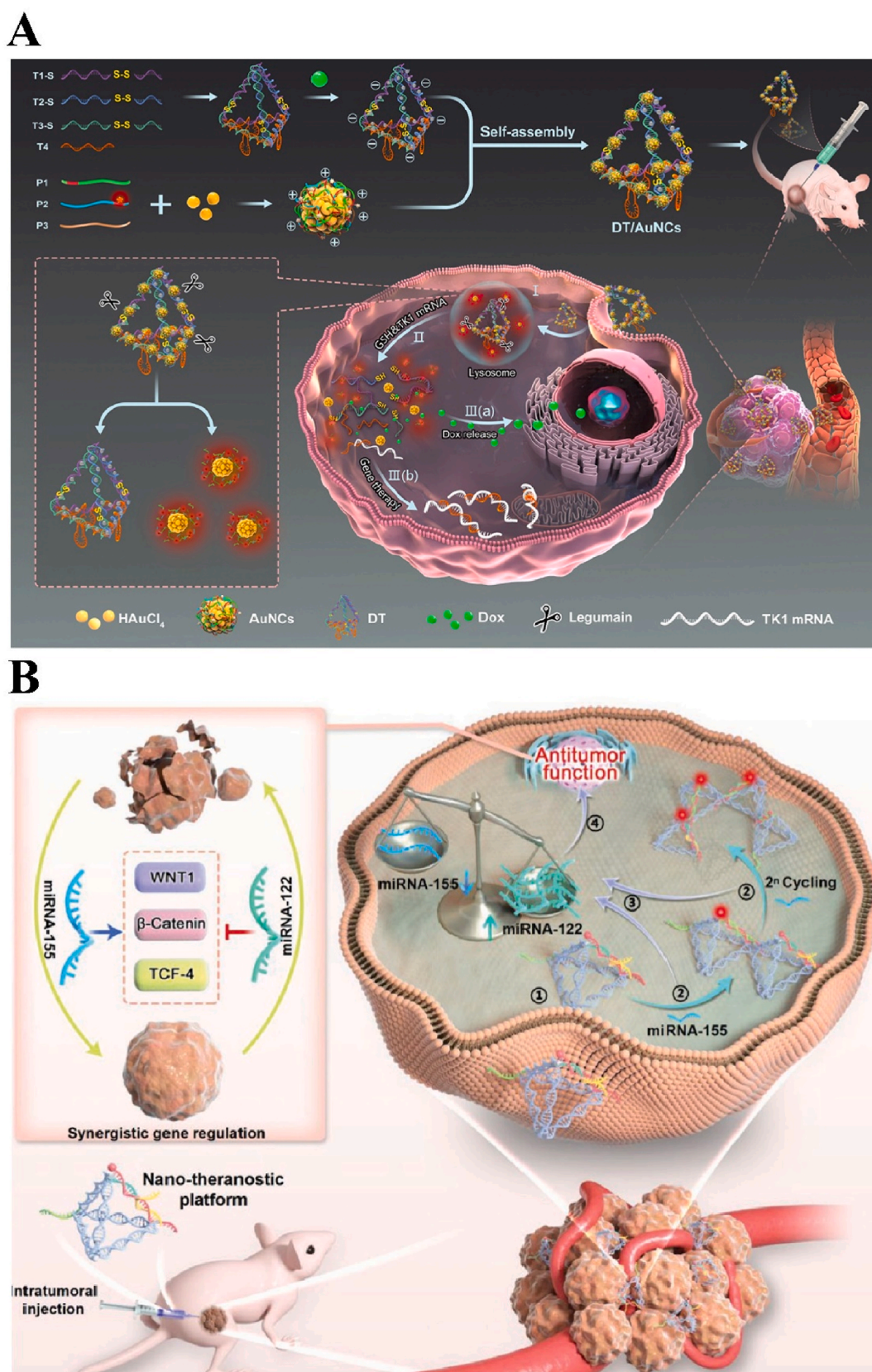


Fig. 15. Schematic illustration of TDN-based theranostics platforms for biomarkers imaging and cancer treatment. (A) A nano-theranostics platform based on TDN and AuNCs for breast cancer imaging and therapy. Reprinted from Ref. [158]. Copyright 2022, Elsevier. (B) A dual-miRNA-guided nanotheranostic system based on TDN for HCC cancer imaging and treatment combination. Reprinted from Ref. [159]. Copyright 2023, John Wiley and Sons.

Remarkably, the TDN classifier demonstrated success in bioanalyzing six biomarkers across three different molecular datatypes, including miRNAs, mRNA, and proteins, achieving highly precise prostate cancer (PCa) diagnosis with an AUC of 100 %. The combination of TDN and classifier offers valuable insights for advancing precise diagnosis and targeted therapy.

In summary, the emergence of three-dimensional nanostructure TDN has paved a new pathway for advancing DNA nanotechnology. Compared to other nanomaterials, such as DNA origami and DNA hydrogels, TDN offers distinct advantages and broader applications due to their unique structural and biomedical properties. For instance, the self-assembly process of DNA origami is intricate and demands high concentrations of metal ions in solution [167]. The stability of DNA hydrogels requires further improvement for effective application in complex matrices [168]. In comparison, TDN can be efficiently synthesized through a straightforward single-step process involving the assembly of four equimolar ssDNAs. Furthermore, TDNs provide remarkable advantages, including controllable structures, enhanced stability, well-defined spatial confinement, and rapid penetration capabilities. And the abundant modification sites of TDN allow the integration of various functional molecules. These features make TDN a highly promising carrier for delivering both nanoprobe and therapeutics to targeted tissues [169,170]. Moreover, TDN itself can act as a biologically functional regulator, demonstrating abilities such as promoting cell proliferation, migration, osteogenic differentiation, as well as exhibiting anti-inflammatory and antioxidant effects [171,172]. Consequently, TDN has been utilized across various biological fields, including biosensing, antitumor and antibacterial therapies, bone repair and regenerative medicine [173,174]. Additionally, the application of FTDN in the simultaneous diagnosis and treatment of diseases further establishes it as a versatile and multifunctional tool for clinical applications [175]. Looking ahead, the integration of multifunctional materials and advanced transduction technologies with FTDN holds great promise for the development of highly sensitive FTDN-based biosensors. Additionally, combining FTDN with microsystems, such as microneedle arrays and microfluidic chips, could pave the way for the creation of wearable and implantable sensors, offering innovative solutions for real-time monitoring and diagnostics. We firmly believe that further advancements can be achieved to broaden the biomedical applications of the FTDN-based biosensors.

CRedit authorship contribution statement

Yun Qiu: Writing – original draft. **Yixing Qiu:** Writing – review & editing, Funding acquisition. **Wenchao Zhou:** Software. **Dai Lu:** Formal analysis. **Huizhen Wang:** Formal analysis. **Bin Li:** Resources. **Bin Liu:** Supervision. **Wei Wang:** Supervision, Funding acquisition, Conceptualization.

Declaration of competing interest

The authors declare that they have no known competing financial interests or personal relationships that could have appeared to influence the work reported in this paper.

Acknowledgements

This work was financially supported by National Natural Science Foundation of China [Grant No. 82405012], Hunan Department of Science and Technology [Grant No. 2023JJ40484], Hunan Provincial Department of Education [Grant No.22B0380], Hunan Provincial Administration of Traditional Chinese Medicine [Grant No. B2023060] and Hunan University of Chinese Medicine [Grant No. 2022XJZKC012].

Data availability

Data will be made available on request.

References

- [1] J.-J. Xu, W.-W. Zhao, S. Song, C. Fan, H.-Y. Chen, Functional nanoprobe for ultrasensitive detection of biomolecules: an update, *Chem. Soc. Rev.* 43 (2014) 1601–1611.
- [2] W.F. de Oliveira, P.M. dos Santos Silva, L.C.B.B. Coelho, M.T. dos Santos Correia, Biomarkers, biosensors and biomedicine, *Curr. Med. Chem.* 27 (2020) 3519–3533.
- [3] Y. Zhao, X. Zuo, Q. Li, F. Chen, Y.-R. Chen, J. Deng, D. Han, C. Hao, F. Huang, Y. Huang, *Nucleic acids analysis, Sci. China Chem.* 64 (2021) 171–203.
- [4] V. Vanova, K. Mitrevska, V. Milosavljevic, D. Hynek, L. Richtera, V. Adam, Peptide-based electrochemical biosensors utilized for protein detection, *Biosens. Bioelectron.* 180 (2021) 113087.
- [5] R. Xu, L. Abune, B. Davis, L. Ouyang, G. Zhang, Y. Wang, J. Zhe, Ultrasensitive detection of small biomolecules using aptamer-based molecular recognition and nanoparticle counting, *Biosens. Bioelectron.* 203 (2022) 114023.
- [6] L. Zhang, M. Chu, C. Ji, J. Tan, Q. Yuan, Preparation, applications, and challenges of functional DNA nanomaterials, *Nano Res.* (2022) 1–18.
- [7] R.P. Goodman, I.A. Schaap, C.F. Tardin, C.M. Erben, R.M. Berry, C.F. Schmidt, A. J. Turberfield, Rapid chiral assembly of rigid DNA building blocks for molecular nanofabrication, *Science* 310 (2005) 1661–1665.
- [8] R.P. Goodman, R.M. Berry, A.J. Turberfield, The single-step synthesis of a DNA tetrahedron, *Chem. Commun.* (2004) 1372–1373.
- [9] H. Ding, J. Li, N. Chen, X. Hu, X. Yang, L. Guo, Q. Li, X. Zuo, L. Wang, Y. Ma, DNA nanostructure-programmed like-charge attraction at the cell-membrane interface, *ACS Cent. Sci.* 4 (2018) 1344–1351.
- [10] Y. Zhang, W. Li, T. Ji, S. Luo, J. Qiu, B. Situ, B. Li, X. Zhang, T. Zhang, W. Wang, Localized DNA tetrahedrons assisted catalytic hairpin assembly for the rapid and sensitive profiling of small extracellular vesicle-associated microRNAs, *J. Nanobiotechnol.* 20 (2022) 503.
- [11] S. Luo, Y. Wu, W. Pan, G. Zhong, B. Situ, B. Li, X. Ye, X. Jiang, W. Li, Y. Zhang, An integrated magneto-fluorescent nanosensor for rapid and sensitive detection of tumor-derived exosomes, *Sens. Actuators, B* 374 (2023) 132792.
- [12] Y. Yang, R. Chen, Y. Guo, J. Zhang, S. Ren, H. Zhou, Z. Gao, A two-color fluorescence sensing strategy based on functionalized tetrahedral DNAzyme nanotweezers for OTA detection, *Talanta* 285 (2024) 127348.
- [13] X. Qu, F. Yang, H. Chen, J. Li, H. Zhang, G. Zhang, L. Li, L. Wang, S. Song, Y. Tian, Bubble-mediated ultrasensitive multiplex detection of metal ions in three-dimensional DNA nanostructure-encoded microchannels, *ACS Appl. Mater. Interfaces* 9 (2017) 16026–16034.
- [14] H. Pei, N. Lu, Y. Wen, S. Song, Y. Liu, H. Yan, C. Fan, A DNA nanostructure-based biomolecular probe carrier platform for electrochemical biosensing, *Adv. Mater.* 22 (2010) 4754–4758.
- [15] H. Zhang, X. Liu, C. Zhang, Y. Xu, J. Su, X. Lu, J. Shi, L. Wang, M.P. Landry, Y. Zhu, A DNA tetrahedral structure-mediated ultrasensitive fluorescent microarray platform for nucleic acid test, *Sens. Actuators, B* 321 (2020) 128538.
- [16] A. Tandon, S.H. Park, DNA structures embedded with functionalized nanomaterials for biophysical applications, *J. Kor. Phys. Soc.* 78 (2021) 449–460.
- [17] M. Lin, J. Wang, G. Zhou, J. Wang, N. Wu, J. Lu, J. Gao, X. Chen, J. Shi, X. Zuo, Programmable engineering of a biosensing interface with tetrahedral DNA nanostructures for ultrasensitive DNA detection, *Angew. Chem. Int. Ed.* 54 (2015) 2151–2155.
- [18] S. Wang, J. Guang, Y. Gao, B. Fan, Y. Liang, J. Pan, L. Li, W. Meng, F. Hu, Fluorescent DNA tetrahedral probe with catalytic hairpin self-assembly reaction for imaging of miR-21 and miR-155 in living cells, *Microchim. Acta* 191 (2024) 462.
- [19] S. Minchin, J. Lodge, Understanding biochemistry: structure and function of nucleic acids, *Essays Biochem.* 63 (2019) 433–456.
- [20] D. Wang, X. Xu, Y. Zhou, H. Li, G. Qi, P. Hu, Y. Jin, Short-chain oligonucleotide detection by glass nanopore using targeting-induced DNA tetrahedron deformation as signal amplifier, *Anal. Chim. Acta* 1063 (2019) 57–63.
- [21] C. Song, X. Jiang, Y. Yang, J. Zhang, S. Larson, Y. Zhao, L. Wang, High-sensitive assay of nucleic acid using tetrahedral DNA probes and DNA concatamers with a surface-enhanced Raman scattering/surface plasmon resonance dual-mode biosensor based on a silver nanorod-covered silver nanohole array, *ACS Appl. Mater. Interfaces* 12 (2020) 31242–31254.
- [22] Y. Huang, S. Zhao, W. Zhang, Q. Duan, Q. Yan, H. Fu, L. Zhong, G. Yi, Multifunctional electrochemical biosensor with “tetrahedral tripods” assisted multiple tandem hairpins assembly for ultra-sensitive detection of target DNA, *RSC Adv.* 11 (2021) 20046–20056.
- [23] H. Liu, J. Luo, L. Fang, H. Huang, J. Deng, J. Huang, S. Zhang, Y. Li, J. Zheng, An electrochemical strategy with tetrahedron rolling circle amplification for ultrasensitive detection of DNA methylation, *Biosens. Bioelectron.* 121 (2018) 47–53.
- [24] X. Chen, J. Huang, S. Zhang, F. Mo, S. Su, Y. Li, L. Fang, J. Deng, H. Huang, Z. Luo, J. Zheng, Electrochemical biosensor for DNA methylation detection through hybridization chain-amplified reaction coupled with a tetrahedral DNA nanostructure, *ACS Appl. Mater. Interfaces* 11 (2019) 3745–3752.

- [25] D. Wang, Y. Chai, Y. Yuan, R. Yuan, Precise regulation of enzyme cascade catalytic efficiency with DNA tetrahedron as scaffold for ultrasensitive electrochemical detection of DNA, *Anal. Chem.* 91 (2019) 3561–3566.
- [26] X. Zha, W. Qin, J. Chen, M. Chen, Q. Zhang, K. He, Y. Liu, W. Liu, Anchoring red blood cell with tetrahedral DNA nanostructure: electrochemical biosensor for the sensitive signage of circulating tumor DNA, *Talanta* 251 (2023) 123793.
- [27] S. Ma, Y. Zhang, Q. Ren, X. Wang, J. Zhu, F. Yin, Z. Li, M. Zhang, Tetrahedral DNA nanostructure based biosensor for high-performance detection of circulating tumor DNA using all-carbon nanotube transistor, *Biosens. Bioelectron.* 197 (2022) 113785.
- [28] Z.H. Nejad, F. Fatemi, S.E.R. Siadat, An outlook on coronavirus disease 2019 detection methods, *J. Pharm. Anal.* 12 (2022) 205–214.
- [29] S. Carinelli, C.X. Ballesteros, M. Marti, S. Alegret, M. Pividori, Electrochemical magneto-actuated biosensor for CD4 count in AIDS diagnosis and monitoring, *Biosens. Bioelectron.* 74 (2015) 974–980.
- [30] J. Chen, M. Wang, C. Zhou, J. Zhang, X. Su, Label-free and dual-mode biosensor for HPV DNA based on DNA/silver nanoclusters and G-quadruplex/hemin DNzyme, *Talanta* 247 (2022) 123554.
- [31] Y. Wu, D. Ji, C. Dai, D. Kong, Y. Chen, L. Wang, M. Guo, Y. Liu, D. Wei, Triple-probe DNA framework-based transistor for SARS-CoV-2 10-in-1 pooled testing, *Nano Lett.* 22 (2022) 3307–3316.
- [32] Z. Fan, B. Yao, Y. Ding, D. Xu, J. Zhao, K. Zhang, Rational engineering the DNA tetrahedrons of dual wavelength ratiometric electrochemiluminescence biosensor for high efficient detection of SARS-CoV-2 RdRp gene by using entry-driven and bipedal DNA walker amplification strategy, *Chem. Eng. J.* 427 (2022) 131686.
- [33] Z. Fan, B. Yao, Y. Ding, J. Zhao, M. Xie, K. Zhang, Entropy-driven amplified electrochemiluminescence biosensor for RdRp gene of SARS-CoV-2 detection with self-assembled DNA tetrahedron scaffolds, *Biosens. Bioelectron.* 178 (2021) 113015.
- [34] P. Khan, J.A. Siddiqui, I. Lakshmanan, A.K. Ganti, R. Sargia, M. Jain, S.K. Batra, M.W. Nasser, RNA-based therapies: a cog in the wheel of lung cancer defense, *Mol. Cancer* 20 (2021) 1–24.
- [35] D. Lu, T. Thum, RNA-based diagnostic and therapeutic strategies for cardiovascular disease, *Nat. Rev. Cardiol.* 16 (2019) 661–674.
- [36] J. Zhang, J. Zhu, F. Guo, J. Jiang, M. Xie, L. Hao, J. Chao, Reusable electrochemiluminescence biosensor based on tetrahedral DNA signal amplification for ultrasensitive detection of microRNAs, *Chem. Commun.* 59 (2023) 6869–6872.
- [37] L. Zhu, J. Ye, S. Wang, M. Yan, Q. Zhu, J. Huang, X. Yang, Dual amplification ratiometric biosensor based on a DNA tetrahedron nanostructure and hybridization chain reaction for the ultrasensitive detection of microRNA-133a, *Chem. Commun.* 55 (2019) 11551–11554.
- [38] W. Nie, Q. Wang, L. Zou, Y. Zheng, X. Liu, X. Yang, K. Wang, Low-fouling surface plasmon resonance sensor for highly sensitive detection of microRNA in a complex matrix based on the DNA tetrahedron, *Anal. Chem.* 90 (2018) 12584–12591.
- [39] Y. Cheng, G. Xue, L. Lan, H. Xu, R. Cheng, Q. Song, C. Li, J. Zhang, G. Huang, Z. Shen, Construction of a 3D rigidified DNA nanodevice for anti-interference and reinforced biosensing by turning nuclease into a catalyst, *Biosens. Bioelectron.* (2023) 115501.
- [40] Y. Xu, J. Da, Q. Lan, J. Luo, Z. Lu, R. Peng, F. Yu, Y. Zha, Engineering DNA tetrahedron as a sensing surface of lateral flow test strips and ratiometric visual detection of exosomal microRNA-150-5p, *Sens. Actuators, B* 393 (2023) 134266.
- [41] Y. Zhang, X. Zhang, B. Situ, Y. Wu, S. Luo, L. Zheng, Y. Qiu, Rapid electrochemical biosensor for sensitive profiling of exosomal microRNA based on multifunctional DNA tetrahedron assisted catalytic hairpin assembly, *Biosens. Bioelectron.* 183 (2021) 113205.
- [42] Y. Xu, C. Wang, G. Liu, X. Zhao, Q. Qian, S. Li, X. Mi, Tetrahedral DNA framework based CRISPR electrochemical biosensor for amplification-free miRNA detection, *Biosens. Bioelectron.* 217 (2022) 114671.
- [43] F. Yin, R. Cai, S. Gui, Y. Zhang, X. Wang, N. Zhou, A portable and quantitative detection of microRNA-21 based on cascade enzymatic reactions with dual signal outputs, *Talanta* 235 (2021) 122802.
- [44] Y. Wang, H. Feng, K. Huang, J. Quan, F. Yu, X. Liu, H. Jiang, X. Wang, Target-triggered hybridization chain reaction for ultrasensitive dual-signal miRNA detection, *Biosens. Bioelectron.* 215 (2022) 114572.
- [45] J. Lu, J. Wang, X. Hu, E. Gyimah, S. Yakubu, K. Wang, X. Wu, Z. Zhang, Electrochemical biosensor based on tetrahedral DNA nanostructures and G-quadruplex-hemin conformation for the ultrasensitive detection of MicroRNA-21 in serum, *Anal. Chem.* 91 (2019) 7353–7359.
- [46] X.-l. Zhang, Z.-h. Yang, Y.-y. Chang, D. Liu, Y.-r. Li, Y.-q. Chai, Y. Zhuo, R. Yuan, Programmable mismatch-fueled high-efficiency DNA signal converter, *Chem. Sci.* 11 (2020) 148–153.
- [47] X.-L. Zhang, S.-S. Li, Y.-J. Liu, W.-W. Liu, L.-Q. Kong, Y.-Q. Chai, X.-L. Luo, R. Yuan, High-efficiency 3D DNA walker immobilized by a DNA tetrahedral nanostructure for fast and ultrasensitive electrochemical detection of MiRNA, *Anal. Chem.* 95 (2023) 4077–4085.
- [48] N. Liu, H. Lu, L. Liu, W. Ni, Q. Yao, G.-J. Zhang, F. Yang, Ultrasensitive exosomal MicroRNA detection with a supercharged DNA framework nanolabel, *Anal. Chem.* 93 (2021) 5917–5923.
- [49] Y. Zheng, L. Chen, X. Yin, F. Lin, Y. Xu, X. Lin, S. Weng, Dual-mode biosensor for femtomolar miRNA-155 detection by electrochemiluminescence and adsorptive stripping voltammetry, *Microchem. J.* 165 (2021) 106091.
- [50] X. Hui, C. Yang, D. Li, X. He, H. Huang, H. Zhou, M. Chen, C. Lee, X. Mu, Infrared plasmonic biosensor with tetrahedral DNA nanostructure as carriers for label-free and ultrasensitive detection of miR-155, *Adv. Sci.* 8 (2021) 2100583.
- [51] S. Liu, J. Wu, M. He, B. Chen, Q. Kang, Y. Xu, X. Yin, B. Hu, DNA tetrahedron-based MNzyme for sensitive detection of microRNA with elemental tagging, *ACS Appl. Mater. Interfaces* 13 (2021) 59076–59084.
- [52] S. Wang, C. Wu, J. Luo, X. Luo, R. Yuan, X. Yang, Target-triggered configuration change of DNA tetrahedron for SERS assay of microRNA 122, *Microchim. Acta* 187 (2020) 1–7.
- [53] Y. Wan, H. Wang, J. Ji, K. Kang, M. Yang, Y. Huang, Y. Su, K. Ma, L. Zhu, S. Deng, Zippering DNA tetrahedral hyperlink for ultrasensitive electrochemical microRNA detection, *Anal. Chem.* 92 (2020) 15137–15144.
- [54] H. Chai, Y. Tang, P. Miao, Tetrahedral DNA supported walking nanomachine for ultrasensitive miRNA detection in cancer cells and serums, *Anal. Chem.* 94 (2022) 9975–9980.
- [55] L. Shan, Y. Chen, X. Tan, S. Ge, L. Zhang, L. Li, J. Yu, L. Li, Tetrahedral DNA nanostructure-engineered paper-based sensor with an enhanced antifouling ability for photoelectrochemical sensing, *Anal. Chem.* 95 (2023) 4760–4767.
- [56] Y. Zhou, H. Wang, H. Zhang, Y. Chai, R. Yuan, Programmable modulation of copper nanoclusters electrochemiluminescence via DNA nanocranes for ultrasensitive detection of microRNA, *Anal. Chem.* 90 (2018) 3543–3549.
- [57] S. Jiang, Q. Li, C. Wang, Y. Pang, Z. Sun, R. Xiao, In situ exosomal microRNA determination by target-triggered SERS and Fe₃O₄@ TiO₂-based exosome accumulation, *ACS Sens.* 6 (2021) 852–862.
- [58] L. Li, Y. Meng, L. Li, S. Wang, J. Ding, W. Zhou, A tetrahedral DNA nanoflare for fluorometric determination of nucleic acids and imaging of microRNA using toehold strands, *Microchim. Acta* 186 (2019) 1–8.
- [59] D. Samanta, S.B. Ebrahimi, C.A. Mirkin, Nucleic-acid structures as intracellular probes for live cells, *Adv. Mater.* 32 (2020) 1901743.
- [60] C. Chen, D.A. Ridzon, A.J. Broomer, Z. Zhou, D.H. Lee, J.T. Nguyen, M. Barbisin, N.L. Xu, V.R. Mahavakar, M.R. Andersen, Real-time quantification of microRNAs by stem-loop RT-PCR, *Nucleic Acids Res.* 33 (2005) e179.
- [61] J. Gao, H. Zhang, Z. Wang, A DNA tetrahedron nanoprobe-based fluorescence resonance energy transfer sensing platform for intracellular tumor-related miRNA detection, *Analyst* 145 (2020) 3535–3542.
- [62] S. Li, C. Wang, Y. Xu, W. Wang, X. Zhao, Q. Qian, X. Mi, A designer DNA tetrahedron-based molecular beacon for tumor-related microRNA fluorescence imaging in living cells, *Analyst* 147 (2022) 2231–2237.
- [63] W. Zhao, Y. Jiang, H. Zhou, S. Zhang, Hairpin-functionalized DNA tetrahedra for miRNA imaging in living cells via self-assembly to form dendrimers, *Analyst* 147 (2022) 2074–2079.
- [64] C. Xing, Z. Chen, Y. Lin, M. Wang, X. Xu, J. Dai, J. Wang, C. Lu, Accelerated DNA tetrahedron-based molecular beacon for efficient microRNA imaging in living cells, *Chem. Commun.* 57 (2021) 3251–3254.
- [65] L. Mo, D. Liang, W. He, C. Yang, W. Lin, Ratiometric and amplified fluorescence nanosensor based on a DNA tetrahedron for miRNA imaging in living cells, *J. Mater. Chem. B* 9 (2021) 8341–8347.
- [66] S. Bai, B. Xu, Y. Guo, J. Qiu, W. Yu, G. Xie, High-Discrimination factor nanosensor based on tetrahedral DNA nanostructures and gold nanoparticles for detection of MiRNA-21 in live cells, *Theranostics* 8 (2018) 2424.
- [67] Y. Wang, Y. Bai, L.P. Cao, L.L. Li, L. Zhan, H. Zuo, C.M. Li, C.Z. Huang, Catalytic hairpin assembled polymeric tetrahedral DNA frameworks for MicroRNA imaging in live cells, *Biosens. Bioelectron.* 197 (2022) 113783.
- [68] B. Zhang, T. Tian, D. Xiao, S. Gao, X. Cai, Y. Lin, Facilitating in situ tumor imaging with a tetrahedral DNA framework-enhanced hybridization chain reaction probe, *Adv. Funct. Mater.* 32 (2022) 2109728.
- [69] C.-Y. Li, B. Zheng, Y.-F. Kang, H.-W. Tang, D.-W. Pang, Integrating 808 nm light-excited upconversion luminescence powering with DNA tetrahedron protection: an exceptionally precise and stable nanomachine for intracellular MicroRNA tracing, *ACS Sens.* 5 (2019) 199–207.
- [70] L. Yu, S. Yang, Z. Liu, X. Qiu, X. Tang, S. Zhao, H. Xu, M. Gao, J. Bao, L. Zhang, Programming a DNA tetrahedral nanomachine as an integrative tool for intracellular microRNA biosensing and stimulus-unlocked target regulation, *Mater. Today Bio* (2022) 100276.
- [71] H. Schwarzenbach, D.S. Hoon, K. Pantel, Cell-free nucleic acids as biomarkers in cancer patients, *Nat. Rev. Cancer* 11 (2011) 426–437.
- [72] L. He, D.-Q. Lu, H. Liang, S. Xie, C. Luo, M. Hu, L. Xu, X. Zhang, W. Tan, Fluorescence resonance energy transfer-based DNA tetrahedron nanotweezer for highly reliable detection of tumor-related mRNA in living cells, *ACS Nano* 11 (2017) 4060–4066.
- [73] M. He, M. He, J. Zhang, C. Liu, Q. Pan, J. Yi, T. Chen, A spatial-confinement hairpin cascade reaction-based DNA tetrahedral amplifier for mRNA imaging in live cells, *Talanta* 207 (2020) 120287.
- [74] Y. Wan, N. Zhu, Y. Lu, P.K. Wong, DNA transformer for visualizing endogenous RNA dynamics in live cells, *Anal. Chem.* 91 (2019) 2626–2633.
- [75] Z. Qing, J. Hu, J. Xu, Z. Zou, Y. Lei, T. Qing, R. Yang, An intramolecular catalytic hairpin assembly on a DNA tetrahedron for mRNA imaging in living cells: improving reaction kinetics and signal stability, *Chem. Sci.* 11 (2020) 1985–1990.
- [76] Z. Han, F. Wan, J. Deng, J. Zhao, Y. Li, Y. Yang, Q. Jiang, B. Ding, C. Liu, B. Dai, Ultrasensitive detection of mRNA in extracellular vesicles using DNA tetrahedron-based thermophoretic assay, *Nano Today* 38 (2021) 101203.
- [77] V.S.A. Jayanthi, A.B. Das, U. Saxena, Recent advances in biosensor development for the detection of cancer biomarkers, *Biosens. Bioelectron.* 91 (2017) 15–23.
- [78] D. Ou, D. Sun, X. Lin, Z. Liang, Y. Zhong, Z. Chen, A dual-apptamer-based biosensor for specific detection of breast cancer biomarker HER2 via flower-like nanozymes and DNA nanostructures, *J. Mater. Chem. B* 7 (2019) 3661–3669.

- [79] X. Yu, Y. Cao, Y. Zhao, J. Xia, J. Yang, Y. Xu, J. Zhao, Proximity amplification-enabled electrochemical analysis of tumor-associated glycoprotein biomarkers, *Anal. Chem.* 95 (2023) 15900–15907.
- [80] Z. Liu, S. Lei, L. Zou, G. Li, L. Xu, B. Ye, A label-free and double recognition–amplification novel strategy for sensitive and accurate carcinoembryonic antigen assay, *Biosens. Bioelectron.* 131 (2019) 113–118.
- [81] H. Chai, W. Cheng, L. Xu, H. Gui, J. He, P. Miao, Fabrication of polymeric ferrocene nanoparticles for electrochemical aptasensing of protein with target-catalyzed hairpin assembly, *Anal. Chem.* 91 (2019) 9940–9945.
- [82] Z. Fan, Z. Lin, Z. Wang, J. Wang, M. Xie, J. Zhao, K. Zhang, W. Huang, Dual-wavelength electrochemiluminescence ratiometric biosensor for NF- κ B p50 detection with dimethylthiodiaminoterephthalate fluorophore and self-assembled DNA tetrahedron nanostructures probe, *ACS Appl. Mater. Interfaces* 12 (2020) 11409–11418.
- [83] D. Feng, J. Su, Y. Xu, G. He, C. Wang, X. Wang, T. Pan, X. Ding, X. Mi, DNA tetrahedron-mediated immune-sandwich assay for rapid and sensitive detection of PSA through a microfluidic electrochemical detection system, *Microsyst. Nanoeng.* 7 (2021) 33.
- [84] Y. Zhang, D. Feng, Y. Xu, Z. Yin, W. Dou, U.E. Habiba, C. Pan, Z. Zhang, H. Mou, H. Deng, DNA-based functionalization of two-dimensional MoS₂ FET biosensor for ultrasensitive detection of PSA, *Appl. Surf. Sci.* 548 (2021) 149169.
- [85] P. Miao, Y. Jiang, Y. Wang, J. Yin, Y. Tang, An electrochemical approach capable of prostate specific antigen assay in human serum based on exonuclease-aided target recycling amplification, *Sens. Actuators, B* 257 (2018) 1021–1026.
- [86] G. Liu, T. Zhang, Y. Tang, P. Miao, An ultrasensitive aptasensor for prostate specific antigen assay based on Exonuclease T-aided cyclic cleavage, *Sci. China Chem.* 61 (2018) 393–396.
- [87] D. Chen, D. Wang, X. Hu, G. Long, Y. Zhang, L. Zhou, A DNA nanostructured biosensor for electrochemical analysis of HER2 using bioconjugate of GNR@ Pd SSS—apt—HRP, *Sens. Actuators, B* 296 (2019) 126650.
- [88] Z.-W. Wu, X.-C. Xie, H.-R. Guo, H. Xia, K.-J. Huang, A highly sensitive electrochemical biosensor for protein based on a tetrahedral DNA probe, N-and P-co-doped graphene, and rolling circle amplification, *Anal. Bioanal. Chem.* 412 (2020) 915–922.
- [89] Y.-X. Chen, K.-J. Huang, L.-L. He, Y.-H. Wang, Tetrahedral DNA probe coupling with hybridization chain reaction for competitive thrombin aptasensor, *Biosens. Bioelectron.* 100 (2018) 274–281.
- [90] F.-T. Xie, X.-L. Zhao, K.-N. Chi, T. Yang, R. Hu, Y.-H. Yang, Fe-MOFs as signal probes coupling with DNA tetrahedral nanostructures for construction of ratiometric electrochemical aptasensor, *Anal. Chim. Acta* 1135 (2020) 123–131.
- [91] F.-T. Xie, Y.-L. Li, Y. Guan, J.-W. Liu, T. Yang, G.-J. Mao, Y. Wu, Y.-H. Yang, R. Hu, Ultrasensitive dual-signal electrochemical ratiometric aptasensor based on Co-MOFs with intrinsic self-calibration property for Mucin 1, *Anal. Chim. Acta* 1225 (2022) 340219.
- [92] B. Jiang, T. Zhang, S. Liu, Y. Sheng, J. Hu, Polydopamine-assisted aptamer-carrying tetrahedral DNA microelectrode sensor for ultrasensitive electrochemical detection of exosomes, *J. Nanobiotechnol.* 22 (2024) 55.
- [93] C. Wang, Y. Xu, X. Zhao, S. Li, Q. Qian, W. Wang, X. Mi, A double-tetrahedral DNA framework based electrochemical biosensor for ultrasensitive detection and release of circulating tumor cells, *Analyst* 146 (2021) 6474–6481.
- [94] Y. Liu, D. Chen, W. Zhang, Y. Zhang, Mobile DNA tetrahedron on ultra-low adsorption lipid membrane for directional control of cell sensing, *Sens. Actuators, B* 307 (2020) 127570.
- [95] J. Li, Y. Yuan, H. Gan, C. Dong, B. Cao, J.-I. Ni, X. Li, W. Gu, C. Song, L. Wang, Double-tetrahedral DNA probe functionalized Ag nanorod biointerface for effective capture, highly sensitive detection, and nondestructive release of circulating tumor cells, *ACS Appl. Mater. Interfaces* 14 (2022) 32869–32879.
- [96] L. Yang, X. Yin, P. Gai, F. Li, A label-free homogeneous electrochemical cytosensor for the ultrasensitive detection of cancer cells based on multiaptamer-functionalized DNA tetrahedral nanostructures, *Chem. Commun.* 56 (2020) 3883–3886.
- [97] B. Lu, Y. Deng, Y. Peng, Y. Huang, J. Ma, G. Li, Fabrication of a polyvalent aptamer network on an electrode surface for capture and analysis of circulating tumor cells, *Anal. Chem.* 94 (2022) 12822–12827.
- [98] H. Jiang, L.-B. Wang, Y.-T. Zhang, M. Dong, J. Li, J.-D. Wang, An entropy-driven three-dimensional multipedal-DNA walker for ultrasensitive detection of cancer cells, *Anal. Chim. Acta* 1228 (2022) 340299.
- [99] D. Ou, D. Sun, Z. Liang, B. Chen, X. Lin, Z. Chen, A novel cytosensor for capture, detection and release of breast cancer cells based on metal organic framework PCN-224 and DNA tetrahedron linked dual-aptamer, *Sens. Actuators, B* 285 (2019) 398–404.
- [100] C. Wang, Y. Xu, S. Li, Y. Zhou, Q. Qian, Y. Liu, X. Mi, Designer tetrahedral DNA framework-based microfluidic technology for multivalent capture and release of circulating tumor cells, *Mater. Today Bio* 16 (2022) 100346.
- [101] X. Yue, Y. Qiao, D. Gu, Z. Wu, W. Zhao, X. Li, Y. Yin, W. Zhao, D. Kong, R. Xi, Reliable FRET-ON imaging of telomerase in living cells by a tetrahedral DNA nanoprobe integrated with structure-switchable molecular beacon, *Sens. Actuators, B* 312 (2020) 127943.
- [102] Y. Qiu, W. Dang, J. Fan, T. Zhou, B. Li, Y. Liu, Y. Qin, C. Tong, M. Daniyal, W. Wang, DNzyme and rGO based fluorescence assay for Fpg activity analysis, drug screening, and bacterial imaging, *Talanta* 218 (2020) 121158.
- [103] X. Luan, X. Tang, J. Deng, Y. Yang, J. Zhai, T. Luan, Fluorescent nucleic acid probes for DNA repair enzymes: design strategies and applications, *TrAC, Trends Anal. Chem.* 171 (2024) 117489.
- [104] X.-M. Zhou, Y. Zhuo, R. Yuan, Y.-Q. Chai, Target-mediated self-assembly of DNA networks for sensitive detection and intracellular imaging of APE1 in living cells, *Chem. Sci.* 14 (2023) 2318–2324.
- [105] X. Zhou, M. Zhao, X. Duan, B. Guo, W. Cheng, S. Ding, H. Ju, Collapse of DNA tetrahedron nanostructure for “off-on” fluorescence detection of DNA methyltransferase activity, *ACS Appl. Mater. Interfaces* 9 (2017) 40087–40093.
- [106] Y. Wu, M. Wu, M. Liu, D. Wang, L. Wang, T. Weng, J. Han, Closing-upon-repair DNA tetrahedron nanoswitch for FRET imaging the repair activity of 8-oxoguanine DNA glycosylase in living cells, *Anal. Chim. Acta* 1196 (2022) 339481.
- [107] X.-M. Zhou, Y. Zhuo, T.-T. Tu, R. Yuan, Y.-Q. Chai, Construction of fast-walking tetrahedral DNA walker with four arms for sensitive detection and intracellular imaging of apurinic/apryrimidinic endonuclease 1, *Anal. Chem.* 94 (2022) 8732–8739.
- [108] Y. Zhang, Y. Deng, C. Wang, L. Li, L. Xu, Y. Yu, X. Su, Probing and regulating the activity of cellular enzymes by using DNA tetrahedron nanostructures, *Chem. Sci.* 10 (2019) 5959–5966.
- [109] Y. Wu, M. Wu, Q. Wang, J. Han, M. Liu, “Repaired and initiated” intramolecular DNA circuit enables the amplified imaging of DNA repair enzyme activity in live cells, *Sens. Actuators, B* 390 (2023) 133992.
- [110] R. Zhang, R. Zhang, C. Zhao, X. Xu, A DNA tetrahedron docking assembly for imaging telomerase activity in cancerous cells, *Anal. Chim. Acta* 1193 (2022) 339395.
- [111] R. Zhang, R. Zhang, W. Jiang, X. Xu, A multicolor DNA tetrahedron nanoprobe for analyzing human telomerase in living cells, *Chem. Commun.* 57 (2021) 2188–2191.
- [112] W. Cheng, L. Xiang, K. Adeel, J. Zhang, Y. Sun, Z. Zhang, J. Li, Ultrasensitive fluorescent detection of telomerase activity based on tetrahedral DNA nanostructures as carriers for DNA-templated silver nanoclusters, *Anal. Bioanal. Chem.* 414 (2022) 2431–2438.
- [113] Y. Hu, Q. Xie, L. Chang, X. Tao, C. Tong, B. Liu, W. Wang, A radar-like DNA monitor for RNase H-targeted natural compounds screening and RNase H activity in situ detection, *Analyst* 146 (2021) 5980–5987.
- [114] T. Zhou, R. Luo, Y. Li, J. Fan, Y. Hu, C. Tong, B. Liu, D. Li, Activity assay and intracellular imaging of APE1 assisted with tetrahedral DNA nanostructure modified-dnazyme and molecular beacon, *Sens. Actuators, B* 317 (2020) 128203.
- [115] Y. Huang, W. Zhang, S. Zhao, Z. Xie, S. Chen, G. Yi, Ultra-sensitive detection of DNA N6-adenine methyltransferase based on a 3D tetrahedral fluorescence scaffold assisted by symmetrical double-ring dumbbells, *Anal. Chim. Acta* 1184 (2021) 339018.
- [116] Y. Qiu, B. Liu, W. Zhou, X. Tao, Y. Liu, L. Mao, H. Wang, H. Yuan, Y. Yang, B. Li, Repair-driven DNA tetrahedral nanomachine combined with DNzyme for 8-oxo guanine DNA glycosylase activity assay, drug screening and intracellular imaging, *Analyst* 149 (2024) 537–545.
- [117] Y. Han, Y. Wang, F. Zhou, Y. Jiang, F. Liu, Molecular beacon-based DNA tetrahedrons for APE 1 activity detection in living cells, *Sens. Actuators, B* 355 (2022) 131258.
- [118] C. Tong, Y. Hu, Q. Xie, T. Zhou, J. Fan, Y. Qin, B. Liu, W. Wang, Sensitive RNase A detection and intracellular imaging using a natural compound-assisted tetrahedral DNA nanoprobe, *Chem. Commun.* 56 (2020) 3229–3232.
- [119] Q. Xue, R. Guo, Y. Wen, L. Wang, X. Cheng, G. Liu, Q. Wu, Development of a fluorescence-based DNzyme biosensor to detect Pb²⁺ in tobacco leaf extracts for cleaner crop production, *J. Cleaner Prod.* (2022) 132544.
- [120] Y. Li, K. Liu, B. Wang, Z. Liu, C. Yang, J. Wang, X. Ma, H. Li, C. Sun, Engineering DNzyme strategies for fluorescent detection of lead ions based on RNA cleavage-propelled signal amplification, *J. Hazard Mater.* 440 (2022) 129712.
- [121] X. Guo, M. Li, R. Zhao, Y. Yang, R. Wang, F. Wu, L. Jia, Y. Zhang, L. Wang, Z. Qu, Structural and positional impact on DNzyme-based electrochemical sensors for metal ions, *Nanomed. Nanotechnol. Biol. Med.* 21 (2019) 102035.
- [122] H. Guan, S. Yang, C. Zheng, L. Zhu, S. Sun, M. Guo, X. Hu, X. Huang, L. Wang, Z. Shen, DNzyme-based sensing probe protected by DNA tetrahedron from nuclease degradation for the detection of lead ions, *Talanta* 233 (2021) 122543.
- [123] S. Zhao, J. Xiao, H. Wang, L. Li, K. Wang, J. Lv, Z. Zhang, Rapid heavy metal sensing platform: a case of triple signal amplification strategy for the sensitive detection of serum copper, *Anal. Chim. Acta* 1181 (2021) 338908.
- [124] P. Ji, G. Han, Y. Huang, H. Jiang, Q. Zhou, X. Liu, D. Kong, Ultrasensitive ratiometric detection of Pb²⁺ using DNA tetrahedron-mediated hyperbranched hybridization chain reaction, *Anal. Chim. Acta* 1147 (2021) 170–177.
- [125] X. Fu, H. Lin, J. Qi, F. Li, Y. Chen, B. Li, L. Chen, A tetrahedral DNA nanostructure functionalized paper-based platform for ultrasensitive colorimetric mercury detection, *Sens. Actuators, B* 362 (2022) 131830.
- [126] C.-Y. Hong, X.-X. Zhang, C.-Y. Dai, C.-Y. Wu, Z.-Y. Huang, Highly sensitive detection of multiple antibiotics based on DNA tetrahedron nanostructure-functionalized magnetic beads, *Anal. Chim. Acta* 1120 (2020) 50–58.
- [127] C. Hong, X. Zhang, S. Ye, H. Yang, Z. Huang, D. Yang, R. Cai, W. Tan, Aptamer-pendant DNA tetrahedron nanostructure probe for ultrasensitive detection of tetracycline by coupling target-triggered rolling circle amplification, *ACS Appl. Mater. Interfaces* 13 (2021) 19695–19700.
- [128] L. Hao, M. Li, K. Peng, T. Ye, X. Wu, M. Yuan, H. Cao, F. Yin, H. Gu, F. Xu, Fluorescence resonance energy transfer aptasensor of ochratoxin A constructed based on gold nanorods and DNA tetrahedrons, *J. Agric. Food Chem.* 70 (2022) 10662–10668.
- [129] B. He, X. Lu, An electrochemical aptasensor based on tetrahedral DNA nanostructures as a signal probe carrier platform for sensitive detection of patulin, *Anal. Chim. Acta* 1138 (2020) 123–131.

- [130] X. Chen, Z. Guo, Y. Tang, Y. Shen, P. Miao, A highly sensitive gold nanoparticle-based electrochemical aptasensor for theophylline detection, *Anal. Chim. Acta* 999 (2018) 54–59.
- [131] Z. Liu, S. Lei, L. Zou, G. Li, L. Xu, B. Ye, Highly ordered 3D electrochemical DNA biosensor based on dual orientation controlled rolling motor and graftable tetrahedron DNA, *Biosens. Bioelectron.* 147 (2020) 111759.
- [132] C. Jing, H. Chen, R. Cai, Y. Tian, N. Zhou, An electrochemical aptasensor for ATP based on a configuration-switchable tetrahedral DNA nanostructure, *Anal. Methods* 12 (2020) 3285–3289.
- [133] Y. Liu, H. Bian, Y. Wu, Y. Yin, J. Wu, Z. Peng, J. Du, Ultrasensitive electrochemiluminescence biosensors based on programmable aptazyme-induced hybridization chain reaction for detecting adenosine triphosphate and quinine, *Sens. Actuators, B* 369 (2022) 132266.
- [134] S. Yang, Z. Zhao, B. Wang, L. Feng, J. Luo, R. Deng, J. Sheng, X. Gao, S. Xie, M. Chen, Modular engineering of a DNA tetrahedron-based nanomachine for ultrasensitive detection of intracellular bioactive small molecules, *ACS Appl. Mater. Interfaces* 15 (2023) 23662–23670.
- [135] S. Yin, M.N. Hossain, Y. Li, C. Sun, H.-B. Kraatz, Development of a novel electrochemical aptasensor based on catalytic hairpin assembly and DNA tetrahedron for the detection of 25-hydroxyvitamin D3, *Sens. Actuators, B* 354 (2022) 131217.
- [136] R. Zhang, R. Chen, Y. Ma, J. Liang, S. Ren, Z. Gao, Application of DNA Nanotweezers in biosensing: nanoarchitectonics and advanced challenges, *Biosens. Bioelectron.* 237 (2023) 115445.
- [137] X. Wang, J. Wu, W. Mao, X. He, L. Ruan, J. Zhu, P. Shu, Z. Zhang, B. Jiang, X. Zhang, A tetrahedral DNA nanostructure-decorated electrochemical platform for simple and ultrasensitive EGFR genotyping of plasma ctDNA, *Analyst* 145 (2020) 4671–4679.
- [138] N. Li, M. Wang, X. Gao, Z. Yu, W. Pan, H. Wang, B. Tang, A DNA tetrahedron nanoprobe with controlled distance of dyes for multiple detection in living cells and in vivo, *Anal. Chem.* 89 (2017) 6670–6677.
- [139] C. Zhu, J. Yang, J. Zheng, S. Chen, F. Huang, R. Yang, Triplex-functionalized DNA tetrahedral nanoprobe for imaging of intracellular pH and tumor-related messenger RNA, *Anal. Chem.* 91 (2019) 15599–15607.
- [140] S. Xu, Y. Chang, Z. Wu, Y. Li, R. Yuan, Y. Chai, One DNA circle capture probe with multiple target recognition domains for simultaneous electrochemical detection of miRNA-21 and miRNA-155, *Biosens. Bioelectron.* 149 (2020) 111848.
- [141] J. Zhou, F. Liu, Y. Han, H. Li, S. Wei, Y. Ouyang, Y. Chai, R. Yuan, Orderly aggregated catalytic hairpin assembly for synchronous ultrasensitive detecting and high-efficiency Co-localization imaging of dual-miRNAs in living cells, *Anal. Chem.* 95 (2023) 14558–14565.
- [142] L. Mo, D. Liang, M. Mo, C. Yang, W. Lin, Dual-detection of miRNAs in living cells via hybridization chain reaction on DNA tetrahedron, *Sens. Actuators, B* 375 (2023) 132955.
- [143] C. Jiang, F. Meng, D. Mao, Y. Tang, P. Miao, Tetrahedral DNA nanoconjugates for simultaneous measurement of telomerase activity and miRNA, *Chembiochem* 22 (2021) 1302–1306.
- [144] J. Wang, K. Wang, H. Peng, Z. Zhang, Z. Yang, M. Song, G. Jiang, Entropy-driven three-dimensional DNA nanofireworks for simultaneous real-time imaging of telomerase and MicroRNA in living cells, *Anal. Chem.* 95 (2023) 4138–4146.
- [145] C. Yang, Y. Shi, Y. Zhang, J. He, M. Li, W. Huang, R. Yuan, W. Xu, Modular DNA tetrahedron nanomachine-guided dual-responsive hybridization chain reactions for discernible bivariate assay and cell imaging, *Anal. Chem.* 95 (2023) 10337–10345.
- [146] L.L. Li, W.Y. Lv, Y.T. Xu, Y.F. Li, C.M. Li, C.Z. Huang, DNA logic nanodevices for the sequential imaging of cancer markers through localized catalytic hairpin assembly reaction, *Anal. Chem.* 94 (2022) 4399–4406.
- [147] C.H. Li, W.Y. Lv, F.F. Yang, S.J. Zhen, C.Z. Huang, Simultaneous imaging of dual microRNAs in cancer cells through catalytic hairpin assembly on a DNA tetrahedron, *ACS Appl. Mater. Interfaces* 14 (2022) 12059–12067.
- [148] X. Huang, M. Chen, Z. Huang, Y. Zhang, T. Shen, Y. Shi, Y. Tong, X. Zou, S.-Y. Liu, J. Guo, On-site-activated transmembrane logic DNA nanodevice enables highly specific imaging of cancer cells by targeting tumor-related nucleolin and intracellular microRNA, *Anal. Chem.* 95 (2023) 14746–14753.
- [149] J. Hu, M.-h. Liu, C.-y. Zhang, Construction of tetrahedral DNA-quantum dot nanostructure with the integration of multistep forster resonance energy transfer for multiplex enzymes assay, *ACS Nano* 13 (2019) 7191–7201.
- [150] L. Zou, Z. Wu, X. Liu, Y. Zheng, W. Mei, Q. Wang, X. Yang, K. Wang, DNA hydrogelation-enhanced imaging ellipsometry for sensing exosomal microRNAs with a tunable detection range, *Anal. Chem.* 92 (2020) 11953–11959.
- [151] S. Wang, M. Xia, J. Liu, S. Zhang, X. Zhang, Simultaneous imaging of three tumor-related mRNAs in living cells with a DNA tetrahedron-based multicolor nanoprobe, *ACS Sens.* 2 (2017) 735–739.
- [152] Z. Zhou, Y.S. Sohn, R. Nechushtai, I. Willner, DNA tetrahedra modules as versatile optical sensing platforms for multiplexed analysis of miRNAs, endonucleases, and aptamer–ligand complexes, *ACS Nano* 14 (2020) 9021–9031.
- [153] H. Zhao, M. Wang, X. Xiong, Y. Liu, X. Chen, Simultaneous fluorescent detection of multiplexed miRNA of liver cancer based on DNA tetrahedron nanotags, *Talanta* 210 (2020) 120677.
- [154] X. Zhao, N. Na, J. Ouyang, Functionalized DNA nanoplatfrom for multi-target simultaneous imaging: establish the atlas of cancer cell species, *Talanta* 267 (2024) 125222.
- [155] J. Su, Y. Ke, N. Maboyi, X. Zhi, S. Yan, F. Li, B. Zhao, X. Jia, S. Song, X. Ding, CRISPR/Cas12a powered DNA framework-supported electrochemical biosensing platform for ultrasensitive nucleic acid analysis, *Small Methods* 5 (2021) 2100935.
- [156] X. Zhan, J. Zhou, Y. Jiang, P. An, B. Luo, F. Lan, B. Ying, Y. Wu, DNA tetrahedron-based CRISPR bioassay for treble-self-amplified and multiplex HPV-DNA detection with elemental tagging, *Biosens. Bioelectron.* 229 (2023) 115229.
- [157] R. Jia, Y. Wang, W. Ma, J. Huang, H. Sun, B. Chen, H. Cheng, X. He, K. Wang, Activatable dual cancer-related RNA imaging and combined gene-chemotherapy through the target-induced intracellular disassembly of functionalized DNA tetrahedron, *Anal. Chem.* 94 (2022) 5937–5945.
- [158] H. Sun, T. Wang, W. Ma, J. Huang, B. Chen, H. Cheng, S. Duan, X. He, L. Jian, K. Wang, A stable DNA Tetrahedra–AuNCs nanohybrid: on-site programmed disassembly for tumor imaging and combination therapy, *Biomaterials* 288 (2022) 121738.
- [159] S. Yang, J. Luo, L. Zhang, L. Feng, Y. He, X. Gao, S. Xie, M. Gao, D. Luo, K. Chang, A smart nano-theranostic platform based on dual-microRNAs guided self-feedback tetrahedral entropy-driven DNA circuit, *Adv. Sci.* 10 (2023) 2301814.
- [160] J. Yan, X. Zhan, Z. Zhang, K. Chen, M. Wang, Y. Sun, B. He, Y. Liang, Tetrahedral DNA nanostructures for effective treatment of cancer: advances and prospects, *J. Nanobiotechnol.* 19 (2021) 1–16.
- [161] L. Liang, J. Li, Q. Li, Q. Huang, J. Shi, H. Yan, C. Fan, Single-particle tracking and modulation of cell entry pathways of a tetrahedral DNA nanostructure in live cells, *Angew. Chem. Int. Ed.* 53 (2014) 7745–7750.
- [162] Y. Shao, J. Zhao, J. Yuan, Y. Zhao, L. Li, Organelle-specific photoactivation of DNA nanosensors for precise profiling of subcellular enzymatic activity, *Angew. Chem.* 133 (2021) 9005–9013.
- [163] L. Li, R. Ma, W. Wang, L. Zhang, J. Li, E. Eltzov, S. Wang, X. Mao, Group-targeting aptamers and aptasensors for simultaneous identification of multiple targets in foods, *TrAC, Trends Anal. Chem.* (2023) 117169.
- [164] Q. Kou, L. Wang, L. Zhang, L. Ma, S. Fu, X. Su, Simulation-assisted localized DNA logical circuits for cancer biomarkers detection and imaging, *Small* 18 (2022) 2205191.
- [165] Y. Pan, R. Weng, L. Zhang, J. Qiu, X. Wang, G. Liao, Z. Qin, L. Zhang, H. Xiao, Y. Qian, Simulation guided intramolecular orthogonal reporters for dissecting cellular oxidative stress and response, *Nano Today* 46 (2022) 101573.
- [166] F. Yin, H. Zhao, S. Lu, J. Shen, M. Li, X. Mao, F. Li, J. Shi, J. Li, B. Dong, DNA-framework-based multidimensional molecular classifiers for cancer diagnosis, *Nat. Nanotechnol.* 18 (2023) 677–686.
- [167] Z. He, K. Shi, J. Li, J. Chao, Self-assembly of DNA origami for nanofabrication, biosensing, drug delivery, and computational storage, *iScience* 26 (2023).
- [168] C. Yan, Y. Hua, J. Guo, P. Miao, Programmable DNA hydrogels construction with functional regulations for biosensing applications, *TrAC, Trends Anal. Chem.* (2024) 117628.
- [169] S. Li, T. Tian, T. Zhang, Y. Lin, X. Cai, A bioswitchable delivery system for microRNA therapeutics based on a tetrahedral DNA nanostructure, *Nat. Protoc.* (2024) 1–27.
- [170] L. Yao, G. Zhang, Y. Wang, Z. Liu, J. Liang, J. Sun, S. Li, T. Tian, Y. Lin, Development of an inhalable DNA tetrahedron MicroRNA sponge, *Adv. Mater.* (2024) 2414336.
- [171] Q. Zhang, S. Lin, S. Shi, T. Zhang, Q. Ma, T. Tian, T. Zhou, X. Cai, Y. Lin, Anti-inflammatory and antioxidative effects of tetrahedral DNA nanostructures via the modulation of macrophage responses, *ACS Appl. Mater. Interfaces* 10 (2018) 3421–3430.
- [172] M. Zhou, N. Liu, Q. Zhang, T. Tian, Q. Ma, T. Zhang, X. Cai, Effect of tetrahedral DNA nanostructures on proliferation and osteogenic differentiation of human periodontal ligament stem cells, *Cell Prolif.* 52 (2019) e12566.
- [173] S. Hong, W. Jiang, Q. Ding, K. Lin, C. Zhao, X. Wang, The current progress of tetrahedral DNA nanostructure for antibacterial application and bone tissue regeneration, *Int. J. Nanomed.* (2023) 3761–3780.
- [174] X. Chen, Z. Xu, Y. Gao, Y. Chen, W. Yin, Z. Liu, W. Cui, Y. Li, J. Sun, Y. Yang, Framework nucleic acid-based selective cell catcher for endogenous stem cell recruitment, *Adv. Mater.* (2024) 2406118.
- [175] N. Lin, Y. Ouyang, Y. Qin, O. Karmi, Y.S. Sohn, S. Liu, R. Nechushtai, Y. Zhang, I. Willner, Z. Zhou, Spatially localized entropy-driven evolution of nucleic acid-based constitutional dynamic networks for intracellular imaging and spatiotemporal programmable gene therapy, *J. Am. Chem. Soc.* 146 (2024) 20685–20699.